National Science Challenges

RESILIENCE TO NATURE'S CHALLENGES

Kia manawaroa – Ngā Ākina o Te Ao Tūroa

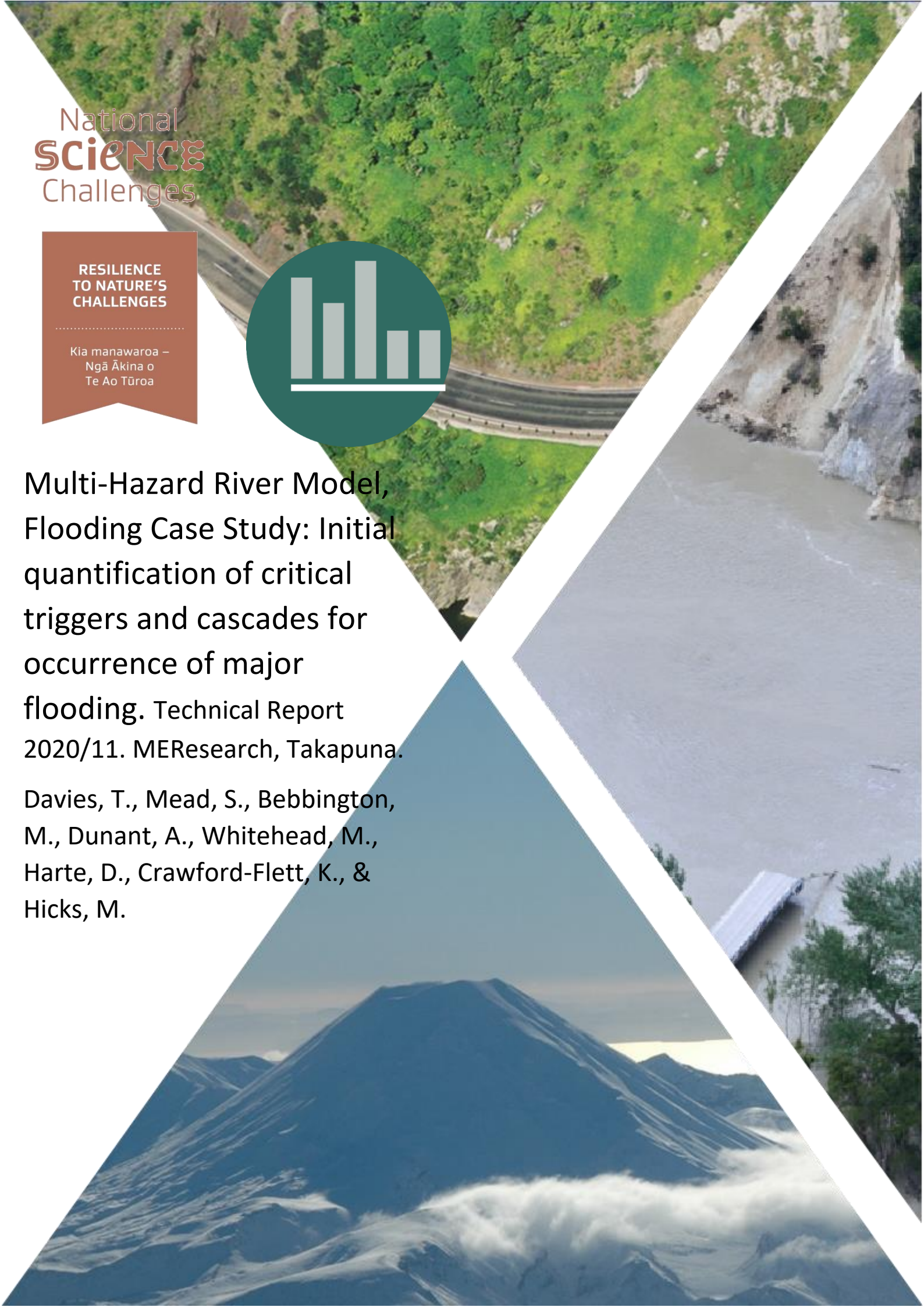

Multi-Hazard River Model, Flooding Case Study: Initial quantification of critical triggers and cascades for occurrence of major flooding. Technical Report 2020/11. MEResearch, Takapuna.

Davies, T., Mead, S., Bebbington, M., Dunant, A., Whitehead, M., Harte, D., Crawford-Flett, K., & Hicks, M.

RESILIENCE TO NATURE'S CHALLENGES | Kia manawaroa – Ngā Ākina o Te Ao Tūroa | National Science Challenges

Resilience to Nature's Challenges 2

Multihazard Risk Model, Flooding Case Study: Initial quantification of critical triggers and cascades for occurrence of major flooding.

Davies, T.[1], Mead, S.[2], Bebbington, M.[2], Dunant, A.[3], Whitehead, M.[2], Harte, D.[4], Crawford-Flett, K.[1], Hicks, M.

1. University of Canterbury, 2. Massey University, 3. GNS Science, 4. Statistics Research Associates

EXECUTIVE SUMMARY

The Case Study is designed to develop a forecastable multihazard scenario environment with a lifespan/forecast horizon of 20-30 years. The purpose is to provide a testbed for multihazard forecasting, impact/operability analysis, economic analysis and decision-making tools. The decadal-scale hazard requires the scenario to be based on a combination of river aggradation, prolonged volcanic activity, and possibly an intense seismic sequence with landsliding. Our previous report identified the Rangitaiki-Tarawera river system as the most suitable location. The Case Study will be initiated by a chosen trigger event; in this case a volcanic eruption and ash deposition event from the Okataina complex. This will be followed by a probabilistically-generated eruption sequence that takes place alongside a probabilistically-generated weather sequence including extra-tropical cyclones. Outburst events from river blockage will also potentially occur. The Case Study will model the impacts of these events on sedimentation and flooding in the Rangitaiki-Tarawera river system, and their consequential impacts on society and the economy both locally and nationally.

The primary hazards that can affect the Rangitaiki-Tarawera river system include volcanic eruption products including tephra deposition, storm rainfall and earthquake shaking; these can cascade into some or all of intensified slope erosion, debris flows, lahars, landslides, landslide dams, dambreak floods, stopbank/levee failure, river aggradation and flooding, the latter two of which can develop and persist for decades with corresponding impacts on infrastructure, societal functions and commerce.

Herein we detail the interrelationships of trigger and consequent or concurrent events that will combine to impact our study area, and outline the process-based model components that will generate a spatiotemporal aggradation and flooding dataset driven by river sedimentation. This will form the basis of further models that will quantify impacts on societal assets and the economic responses and impacts that will follow from these.

List of Abbreviations

Abbreviation	Explanation
BoP	Bay of Plenty
CliFlo	New Zealand's National Climate Database
DEM	Digital Elevation Model
ECMWF	European Centre for Medium-Range Weather Forecasts
MRm	Multihazard Risk model
REC	River Environment Classification
RNC	Resilience to Nature's Challenges Kia manawaroa – Ngā Ākina o Te Ao Tūroa

Glossary

Term	Description
Coseismic	An event or process directly associated with or simultaneously affected by a specific seismic event (earthquake)
Lahar	A gravity driven mass flow containing a mixture of volcanic debris and water, ranging in composition from hyper-concentrated flows (with a high proportion of water) to debris flows (a water-saturated flow containing mostly solids).
Pyroclastic flow	Ground-hugging, hot, multiphase flow of volcanic particles (ash) and gas
Rhyolite	Silica (SiO_2) rich volcanic rock the magma of which is extremely viscous
Plinian eruption	Large explosive eruptions that produce 20 to 35 km-high sustained eruptive ash columns.
Vulcanian eruption	Small to moderate explosive eruptions that produce < 20 km-high short-lived ash columns.

Table of Contents

1. Introduction

The second phase of the MBIE-funded research programme Resilience to Nature's Challenges (RNC2) began on 1 July 2019 and will run until 30 June 2024. This research utilises and extends the outcomes of its predecessors RNC1 (2016-2019) and the Natural Hazards Research Platform (2012-2019). RNC2 has an allocation of $40 million for the 5-year period. High-quality outcome-driven science is expected. RNC2 will run under the same governance and advisory structures as RNC1, continuing the vision:

á b Ŝ ø ½ Ŝ l· f l· y Ř ǎ ă l· y l· ű ǎ ƨ y ƨ Ŧ LJ Ŝ ƨ LJ f Ŝ ø K ƨ K l· Ø Ŝ ű NJ l· y
l· y ű ǎ Ŏ ǎ LJ l· ű Ŝ Σ l· Ř l· LJ ű l· y Ř ű Ŏ K NJ l· ǎ Ø Ŝ ǎ ƴ Ǝ Y Ŏ ű K K l· Ŝ f Ŧ Ŝ l· y Ŏ Ǝ Ŝ Ŝ ă ƨ Ø Ŧ ε y l· ű d

The mission of RNC2 is stated as:

á ² ǎ ű K Ŝ y Ř will co Ř Ŝ ă ǎ Ǝ y l· y Ř LJ NJ ƨ Ř dz Ŏ Ŝ NJ Ŝ ă Ŝ l· NJ Ŏ K ű ƨ l· Ŏ Ŏ Ŝ f
natural hazards resilience.
We will unify underpinning research of geophysical, weather and fire hazard into a multihazard risk model.
We will contribute to economic, social and engineering solutions to build-in Ǝ Ŝ y Ŝ NJ l· ű ǎ ƨ y l· f NJ Ŝ ă

The RNC2 programme comprises ten research themes (Fig. 1): Resilience in Practice, Māori, Urban, Rural, Built; Multihazard Risk, Earthquake-Tsunami, Volcanic, Coastal, Weather.

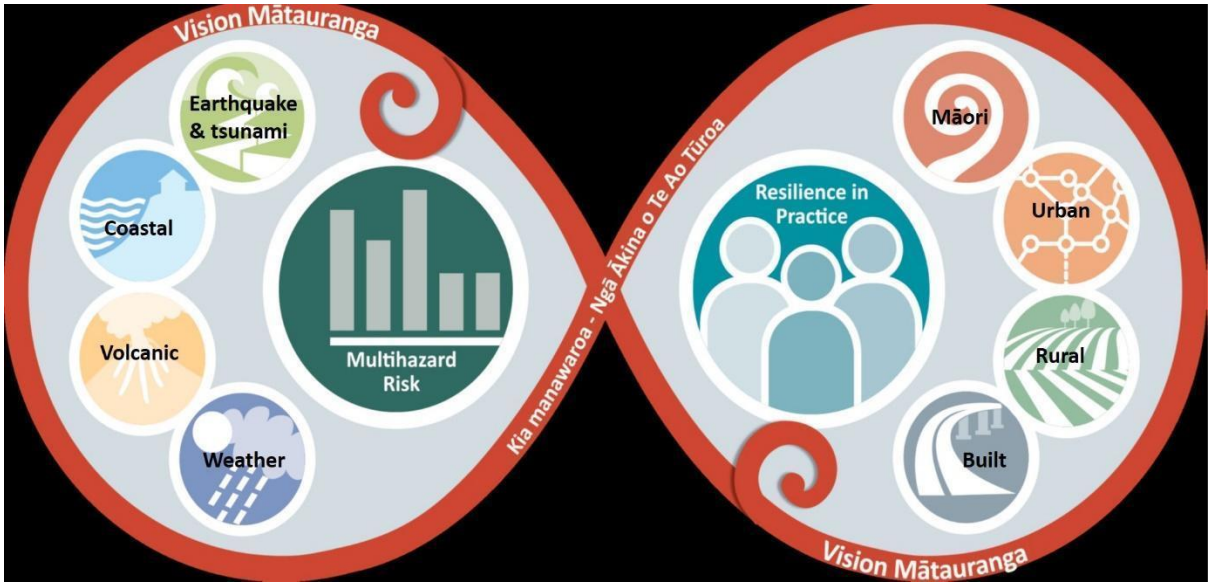

Fig. 1. RNC2 Research programme 2019-2024

In this second report on the Multihazard Risk Model we describe the base data required to characterise the study area; quantify the trigger and subsequent events that alter the landscape in the area; and describe the architecture of the suite of models to be developed and used to generate the spatiotemporal distribution of sedimentary and flooding events and impacts in the study area. This builds on the first report that detailed Case Study requirements and subsequent selection of the Case Study area: the Rangitaiki/Tarawera system (Davies et al, 2020).

2. The Multihazard Risk Model (MRm) theme

This theme (Fig. 2) addresses the issues of modelling coincident and cascading hazards and their impacts, and the estimation of long-term and society-wide social and economic impacts, using realistic scenario frameworks together with improved resilience investment business cases.

The broad outline of the case study models suite is shown in Fig. 2.

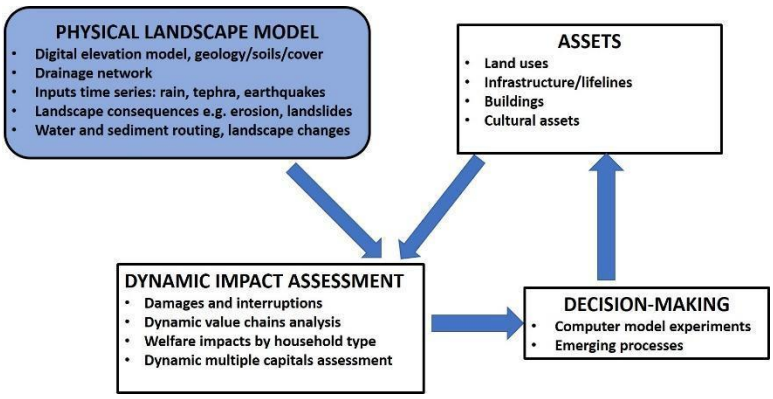

Fig. 2 Conceptual model of Case Study in MRm theme

The end-to-end Case Study is a crucial component of the Multihazard Risk Model Theme of RNC2 as shown in Fig. 3, and intended to serve as a vehicle to develop and test the quantitative modelling suite shown in Fig. 4.

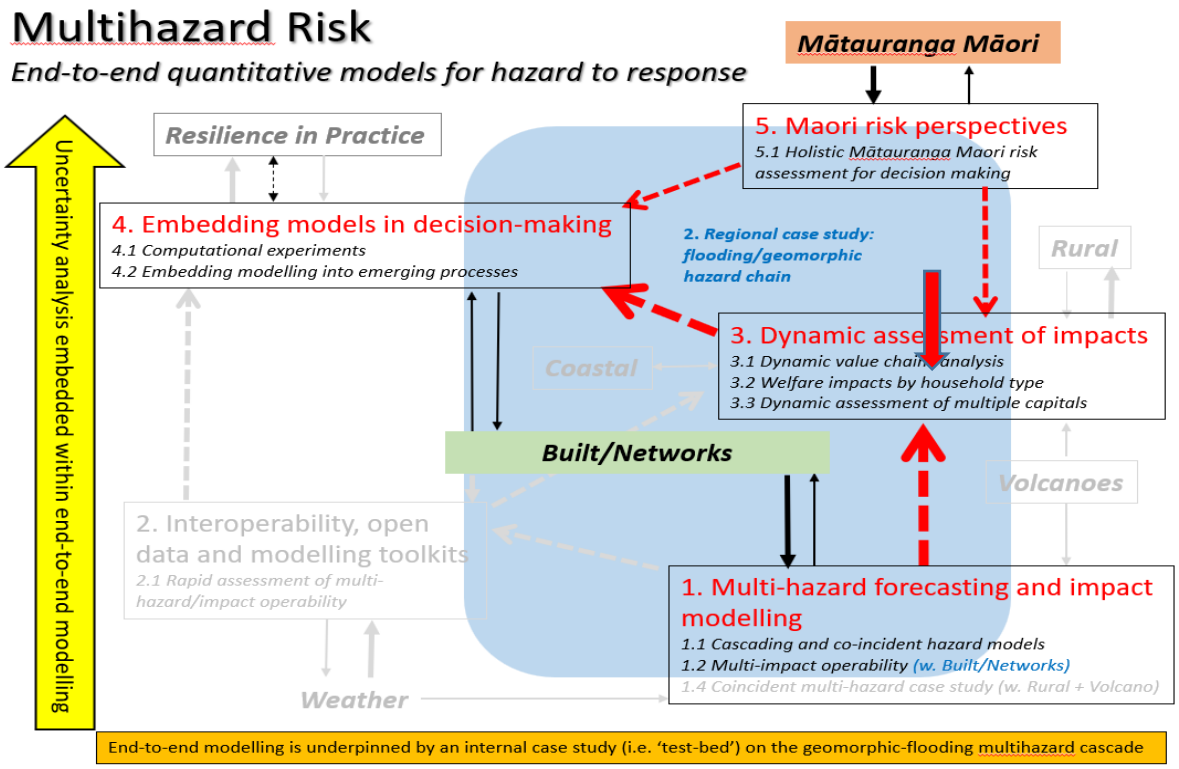

Fig. 3. Multihazard Risk Model Theme of RNC2; centrality of Case Study illustrated by blue area.

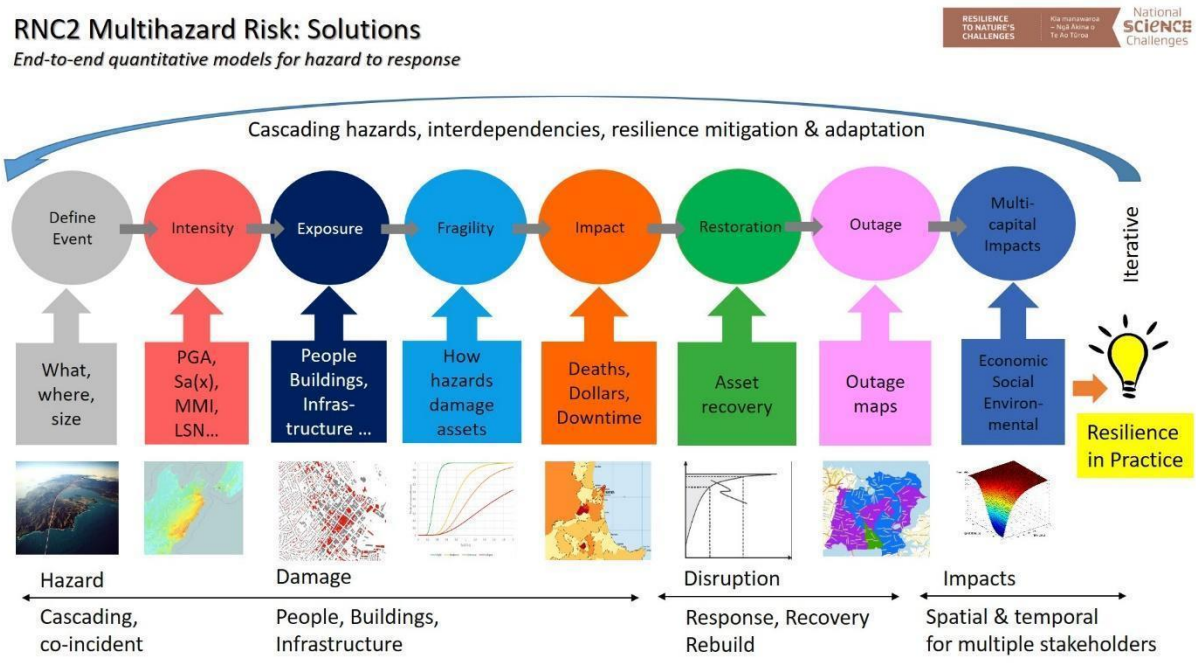

Fig. 4. Example of end-to-end modelling sequence of MRm. Source: GNS Science

The main output of the hazard modelling will be a probabilistically-derived spatiotemporal sequence of river and floodplain aggradation resulting from tephra (volcanic ash) deposits being reworked into and along rivers by rainfall and streamflow. The Case Study deliverables contracted for RNC2 are listed in Table 1; the present report constitutes deliverable 2.1.2.

Table 1. MRm Case Study: Deliverables

2.1.1	River system and potential hazard cascades selected for Case Study. *Deliverable* Report summarizing criteria and reasons for selection of river system and potential hazard cascades. Completed report: Davies et al. (2020)	Tim Davies	Mark Bebbington, Garry McDonald, Stuart Mead, Nicky Smith, Emily Harvey, Charlotte Brown, Garth Harmsworth, Anita Wreford, Ilan Noy, Ryan Paulik, Alex Dunant, David Harte, Melody Whitehead	29 February 2020
2.1.2	**Initial quantification of critical triggers and cascades for occurrence of major flooding.** ***Deliverable*: Report outlining hazard cascades and input data.**	**Tim Davies**	**Alex Dunant, Stuart Mead, Melody Whitehead**	**30 November 2020**
2.1.3	Models developed for sediment transport/deposition and flood depths/extents over time. *Deliverable* Manuscript submitted on modelling river system response to loading.	Tim Davies	PhD student (UC), Alex Dunant, Stuart Mead, Ryan Paulik	31 August 2022
2.1.4	Physical and socio-economic impacts of major flooding quantified. *Deliverable* Report on potential physical and socio-economic impacts of Case Study events	Tim Davies	PhD student (UC), Garry McDonald, Nicky Smith, Ryan Paulik, Stuart Mead, Emily Harvey, Melody Whitehead	30 November 2023
2.1.5	Role of control structures in flooding assessed through multiple capitals.	Tim Davies	PhD student (UC), Garry McDonald, Nicky Smith, Ryan Paulik, Stuart Mead, Emily Harvey, Melody	30 June 2024

	Deliverable Manuscript submitted on effect of flood control structures on societal impacts of super-design events.		Whitehead, Mark Bebbington, Charlotte Brown	

3. MRm Case Study Scenario Framework

The main purpose of the Case Study is to develop and demonstrate capability for multihazard risk modelling and incorporate the modelling of 'decision points' with a particular focus on flooding. While the far-reaching impacts of the volcanic trigger event are not intended as the study focus (e.g. loss of tourism because of fear), we also require realistic scenarios which will be useful to stakeholders. Thus, these aspects should be included as far as possible – but they largely become part of the 'background' that does not change under any decisions.

Conventional flood risk management strategies are based on the increased water levels caused by individual river floods, and modelling of such events is very well developed; by contrast, the longer-term increase in river bed levels caused by a major sediment delivery episode in a river's headwaters will cause increasing flood hazard over a period of decades that may be much more intense and rapid than that caused by normal long-term aggradation caused by landscape evolution. The impacts of this flood hazard will depend on the sequence of storms or periods of prolonged rainfall that occur during this period. Hence, it was decided at an early stage that the hazard cascade for the Case Study would have increased flood hazard as its central output, in order to provide a suitably lengthy impact sequence.

Flooding can be caused by a variety of overlapping or cascading events (rainstorms, aggradation, landslides, volcanic ashfall and their antecedent/consequent hazards where applicable). In the hazard modelling phase of the MRm Case Study, through a mix of computational, graphical, and statistical approaches, we will examine the effects of the spatiotemporal distribution of hazards and the effect of river management structures on aggradation and flood inundation hazards.

The potential hazard cascades that lead to flooding are depicted in Fig. 5. Earthquake-triggered, or "coseismic", landslide-driven flooding has been relatively well studied in South Island contexts (e.g. Briggs et al., 2018; Robinson and Davies, 2013; Robinson et al., 2016; Robinson et al., 2018), but the aggradation and flooding resulting from severe tephra loading on river catchments has not hitherto been modelled. Nevertheless, considerable empirical experience of this process exists through studies of the 1980 Mt St Helens (e.g. Major et al., 2000), 1991 Pinatubo (e.g. Gran and Montgomery, 2005) and 2008 Chaitén (e.g. Pierson et al., 2013) eruptions, and there are studies of the tephra distributions resulting from the c. 5000 BP Whakatane (Kobayashi et al., 2005) and c. 1300 AD Kaharoa (Sahetapy-Engel et al., 2014) eruptions from the Okataina volcanic centre in the central North Island that can underpin scenario development for the Case Study. Hence tephra-driven hazard cascades are preferred to seismically-driven ones, particularly because of the opportunity for scientific advance. Nevertheless eruptions commonly involve earthquakes, and we may include an eruption-related river-blocking mass movement, which could be coseismic, as part of the scenario.

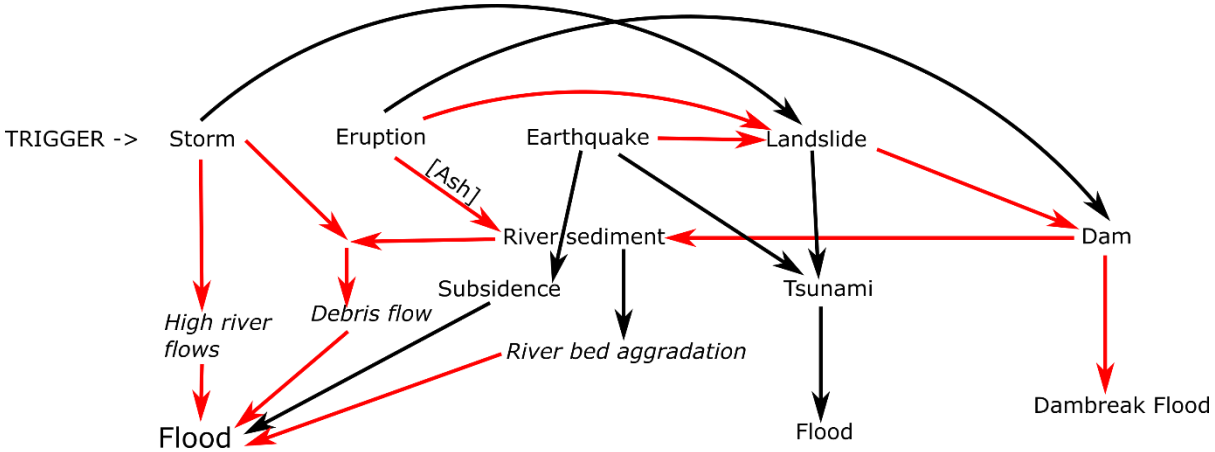

Fig. 5. Potential hazard cascades leading to flooding: red arrows indicate cascades in Case Study

In the end-to-end modelling sequence (Fig. 4), the physical (hazard) components of the MRm cascade scenario affect, and are required to interface with, exposure, impact, fragility and decision-making components which may, in turn, affect elements of the physical hazard cascade. A network outline of the complete MRm framework is shown in Fig. 6, indicating connections between the physical model (green shading) and external models. The internal connections between physical components of the hazard cascade system from Fig. 5 are also highlighted in this network diagram.

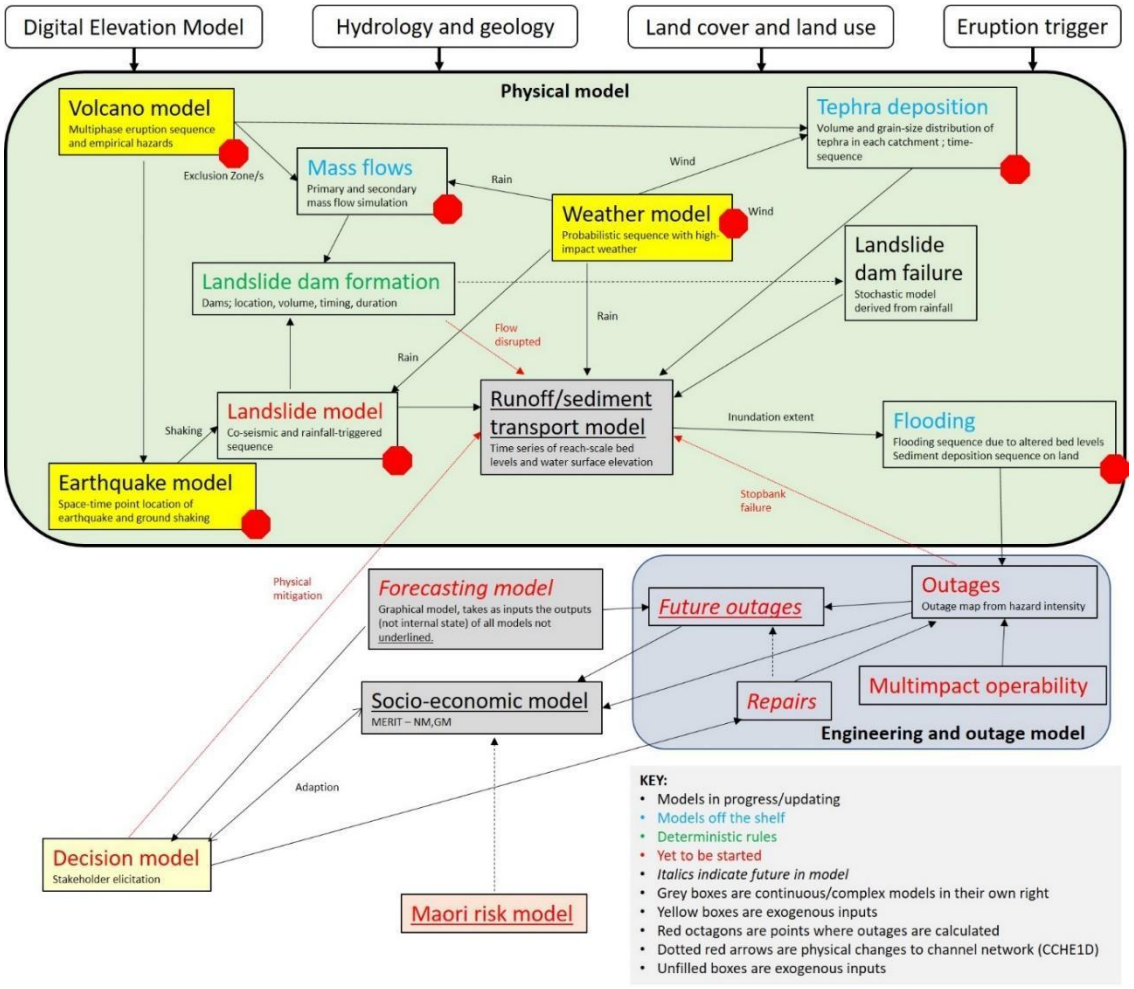

Fig. 6 Complete suite of models for MRm Output

This report focuses on the physical model, outlining the expected inputs, outputs and proposed methodology of each component.

4. River system selection

The river systems of the central North Island were assessed for their potential as Case Study sites as described in the first report of this series (Davies et al., 2020) and the Rangitaiki/ Tarawera system was selected (Fig. 7). This has a total catchment area of 3589 km^2, with about 20% in exotic grassland (pasture), 25% in indigenous forest, 47% in exotic forest and 3.5% in scrub (Fig. 11). The hazard cascades that can occur in this river system are those indicated by the red arrows in Fig. 5.

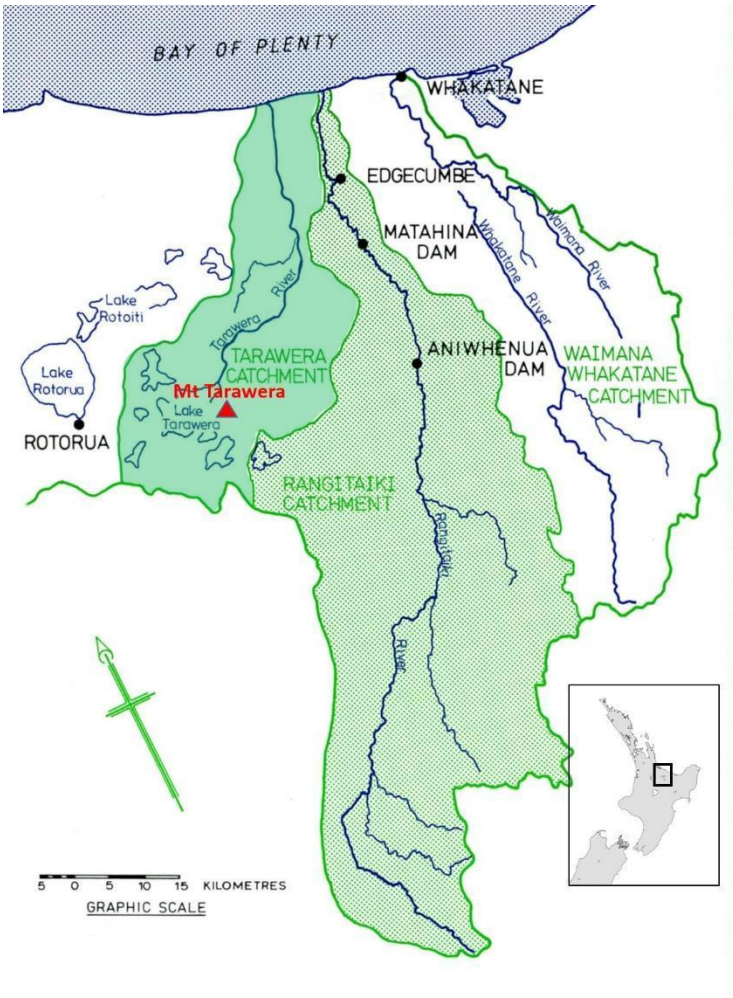

Fig. 7. Rangitaiki-Tarawera River System: Total area 3589 km^2.

5. Input data

5.1 Base data

The suite of base input data for the case study includes a digital elevation model of the river system catchment; the digitised stream system network; land use; soils and geology parameterised by infiltration rates and water table depth; streamflow data for the river system; and water volumes and sedimentation rates in the two dam-related lakes Aniwhenua and Matahina. These are now described in more detail.

5.1.1 DEM

The digital elevation model, shown in Fig. 8, is sourced from BOPLASS Ltd. (https://www.boplass.govt.nz/) and has a 2 m grid size. The bare-ground DEM was created from aerial LiDAR surveys at varied point densities between 2011 and 2013 (generally higher point densities near the coast). This resolution is more than sufficient for purposes of this study and will likely need to be resampled for most modelling on terrain. Terrain statistics for each order 1 catchment were calculated on the original 2 m DEM.

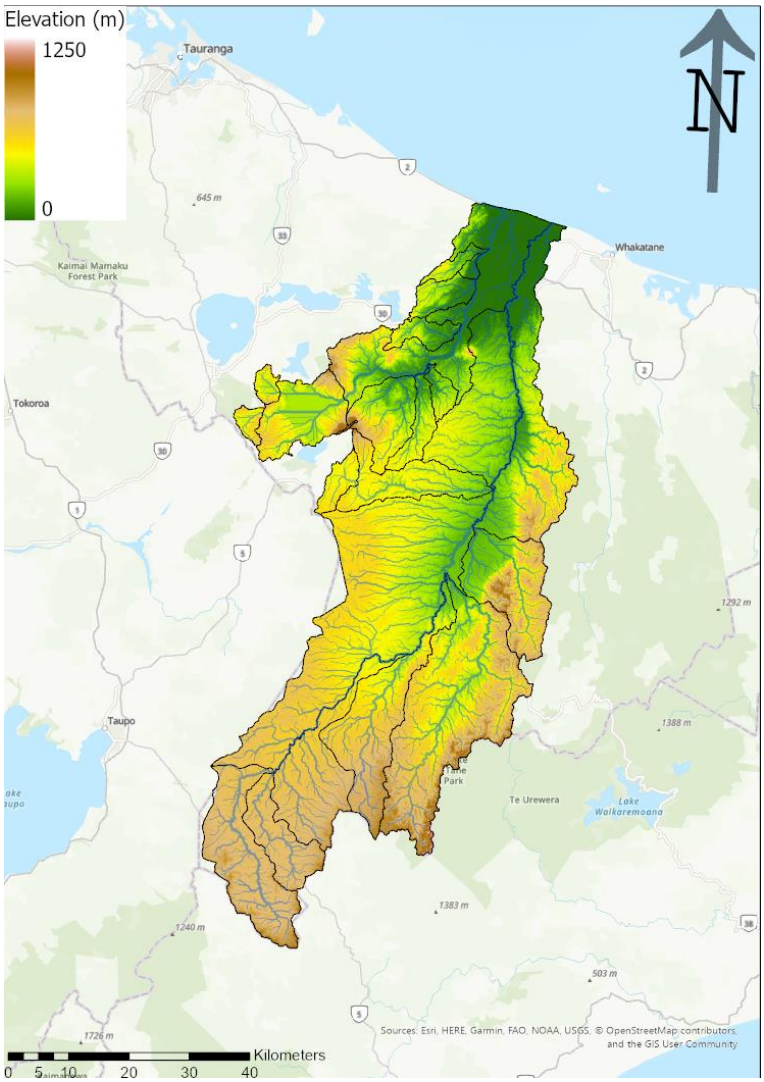

Fig. 8. Digital elevation model for study area.

5.1.2 Hydrology and geology

The stream network and secondary catchments are shown in Fig. 9. The stream network is taken from the NIWA River Environment Classification (REC) 2 (version 5.0), containing catchment attributes, polygons and streamlines for every segment of the Tarawera-Rangitaiki system. The attributes class catchments according to their dominant climate, flow source, geology (e.g. hard soil, soft soil, volcanic soils), land use, location (stream order) and landform/slope. The geology, land use, location and landform attributes may be useful for this study. Full detail of categories and classes is summarised in Snelder et al. (2010). Secondary catchment boundaries and names from Bay of Plenty Regional Council have been merged with the REC database to provide an additional grouping of sub-catchments. The subcatchment boundaries are defined by the primary stream/s feeding the Rangitaiki and Tarawera rivers. These subcatchments have been previously used to model river flow within the catchment (Wallace et al., 2012).

Rainfall, river level and flow for the Rangitaiki-Tarawera catchment system are available from Bay of Plenty Regional council (https://envdata.boprc.govt.nz). The gauges most often used to represent flooding in reports both lie in the Rangitaiki plains (Tarawera at Awakaponga; Rangitaiki at Te Teko). Daily rainfall data are also available from NIWA (https://cliflo.niwa.co.nz/) with nine rainfall gauges within the catchment area and a further four within 10 km. Of these, seven have complete (daily) data for an overlap of at least twenty years.

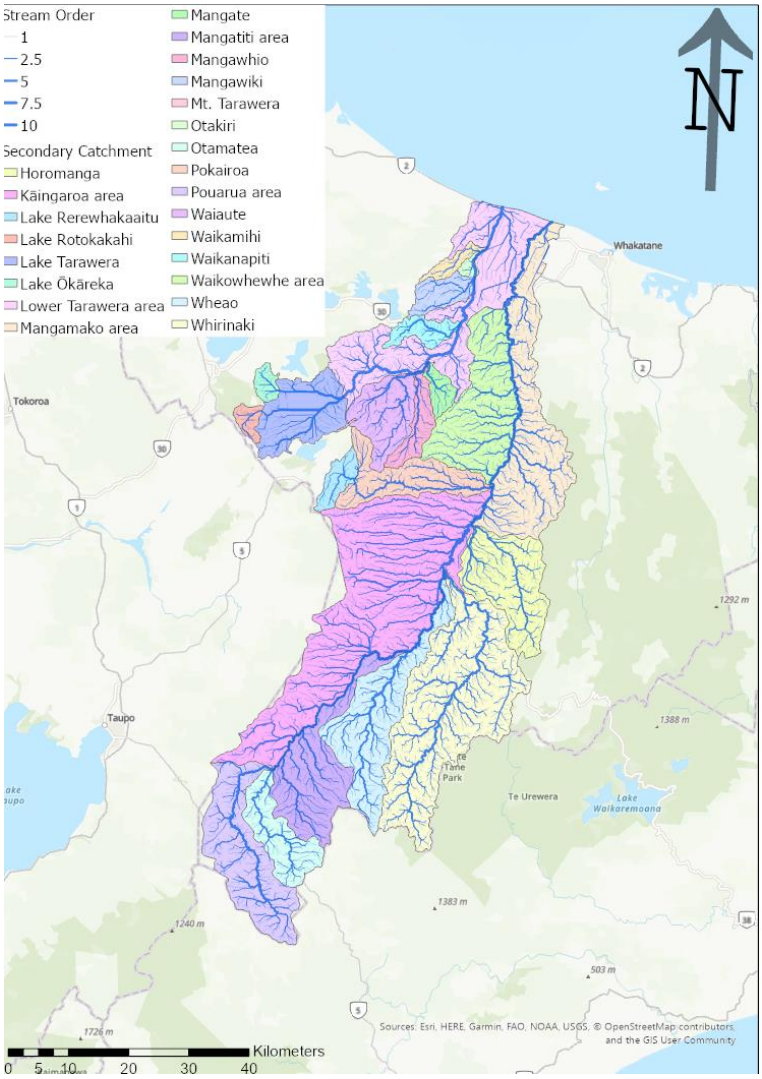

Fig. 9. Streams and sub-catchments within case study area, data sourced from NIWA REC2 and Bay of Plenty Regional Council

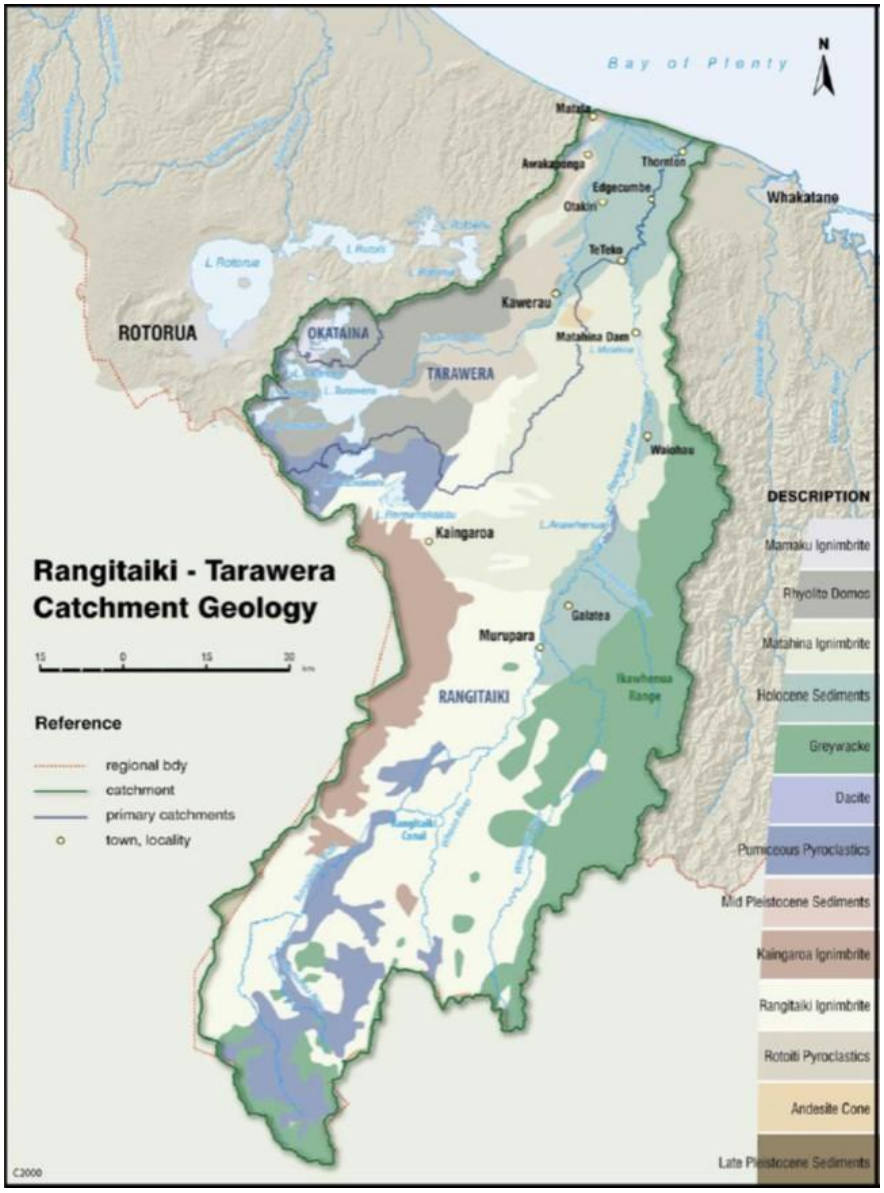

Fig. 10. Geology of the Rangitaiki-Tarawera catchment (Britton, 2008)

Geology of the Tarawera/Rangitaiki catchment is shown in Fig. 10. The Rangitaiki catchment upstream of Murapara is almost homogenous in characteristics with sequences of permeable ash and pumice that regulate much of the runoff and result in smaller flood flows in the upper catchment (Blackwood, 2000; Manville et al., 2005). Below Murapara, the Rangitaiki river passes through the Galatea plains (and the Waiohau Plains below Lake Aniwhenua), containing slower-draining (compared to upstream) volcanic sediments and fluvial sediments delivered from the steep, native-vegetated Ikawhenua Ranges through the Whirinaki and Horomanga Rivers (Pain and Pullar, 1968). The river enters the Rangitaiki plains after travelling through steep gorges and the Aniwhenua and Matahina Dams. The plains consist of drained peat swamps, pumice and recent flood alluvium. The infiltration rates of these soils are still moderately rapid due to the presence of coarse ash (e.g. from the Kaharoa and Tarawera events and the 1800 BP Taupo eruption; Griffiths, 1985). Upstream of the Rangitaiki Plains, the Tarawera catchment contains mostly deep pumice soils which regulate the runoff in a similar way to the upper Rangitaiki catchment (Britton, 2008).

5.1.3 Land use

The regional scale land use map (Fig. 11), from Bay of Plenty Regional Council, is a validated land use map derived from the Land Cover Database v4 and recent aerial imagery. It shows that much of the

catchment is covered by either exotic or native forests with the exception of the Rangitaiki and Galatea plains, which are mostly utilised for dairy and smaller amounts of sheep, beef or horticulture.

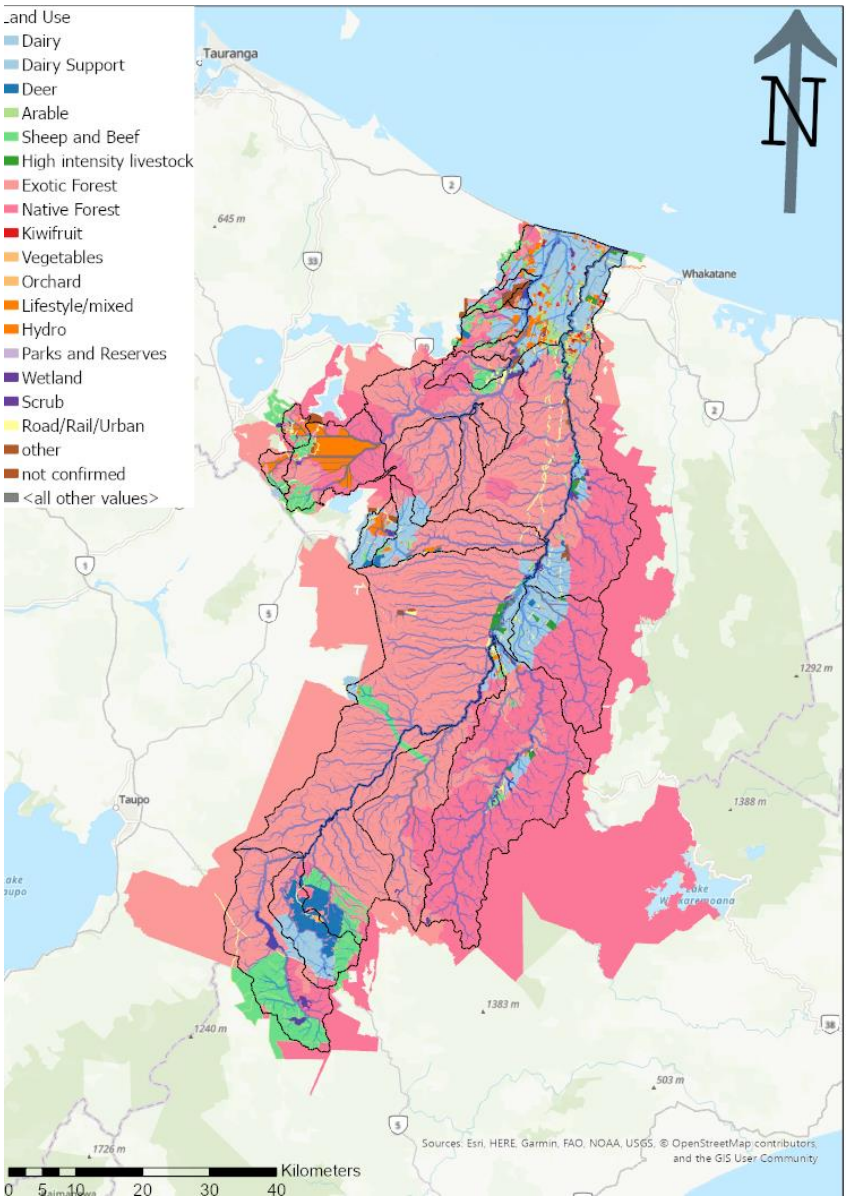

Fig. 11. Land use in the Rangitaiki-Tarawera catchment

5.1.6 Lakes Aniwhenua and Matahina

Lakes Aniwhenua and Matahina (Fig. 7) are formed behind hydro-power dams. The annual average suspended and bed loads delivered to the coast prior to construction of these dams were about 201,000 and 188,000 tonnes respectively (i.e. about 400,000 tonnes total; Phillips and Nelson, 1981). These dropped when the Matahina Dam was built (1967) to only 75,000 tonnes combined. With an initial water storage volume of 55 million m^3, annual deposition in Matahina Lake was estimated at 235,000 m^3 before Aniwhenua Dam was built (Phillips 1980). The much smaller Aniwhenua Dam, 25 km upstream of Matahina, has a water storage capacity of 5 million m^3 and was completed in 1981. During its first 15 years of operation, Lake Aniwhenua accumulated approximately 1.5 million m^3 of sediment, at an annual rate of 100,000 m^3/yr, intercepting sediment that would otherwise have deposited in Lake Matahina. Using these figures, in 2017 the Matahina storage volume should have been reduced to 44 million m^3; in 2040 it will be reduced to just over 42 million m^3. In the context of the present Case study this is the maximum volume of sediment that could potentially be stored in

the lake before excess sediment starts to move downstream onto the Rangitaiki Plains. However, in reality, the lake will begin bypassing sediment with increasing efficiency as its water volume reduces.

Both Āniwaniwa and Matahina Dams form part of an active geomorphological landscape. These dams have experienced movement/deformation and erosion incidents attributed to seismic events that have required engineering remediation (http://www.waterfordpress.co.nz/business/waiotahi-contractors/; Gillon, 2007). Further upsteam in the Rangataiki River catchment, a number of smaller dam and canal structures form the Wheao and Flaxy hydroelectric power scheme. For the purposes of the MRm, these structures are not considered to be major contributors to sediment or water balances.

6. Hazard triggers and cascades

6.1 General

As indicated in Fig. 5, the main triggers of hazards in the Rangitaiki/Tarawera river system investigated for this work are volcanic eruptions, storms and possibly earthquakes. Events are required that impact the system at a regional rather than national level and are not so large that the direct impacts are immediately overwhelming. Examples of suitable volcanic eruptions are thus the c. 5000 BP Whakatane and c. 1300 AD Kaharoa eruptions from the Okataina volcanic centre in the central North Island (the impacts of the Taupo 1800 BP eruption are too large for this case study). The major landscape impact is the widespread deposition of volcanic ash or tephra that can be eroded by subsequent rainstorms and reworked into rivers, giving rise to an aggradation-flooding sequence that moves into the lower river reaches and impacts societal assets and functions. Infrastructure of interest for the Case Study area may include Whakatane airport and runway, roads and railways and their bridges, rail station(s), electricity pylons and powerlines, communication masts, landfills, quarries, cemeteries, river stopbanks and land drainage channels, and key buildings such as dairy manufacturing or timber processing plants.

The trigger event for the Case Study is a multi-year sequence of volcanic phenomena including ashfall, dome-building/collapse and lava extrusion, loosely based on the Kaharoa eruption that involved 13 episodes spread over at least 5 years about 700 years ago (Sahatepy-Engel et al., 2014). The sequence of meteorological events (rainstorms) that drives the motion of sediment through the system over the Case Study time period (several decades) following the trigger eruption is generated on the basis of statistical analysis of past events; these are constrained by local atmospheric circulation parameters over the time-scale of the study. The RNC High Impact Weather programme does not currently include weather variations due to climate change, however, The Deep South (https://www.deepsouthchallenge.co.nz/) – another National Science Challenge - does and their findings may be incorporated into this case study as work progresses in both projects.

Other notable hazard events within the overall cascade include landslides. While the vast majority of landslides that occur during the reworking of tephra by rainfall will be small, and are included in the erosion code due to runoff, a small number of larger landslides may be introduced stochastically to represent the likely proximal effect of eruptive phenomena; for example, it is known that during the Kaharoa eruption a lava flow dammed the Tarawera river and failure of the dam subsequently resulted in a major sedimentation episode down the river (Hodgson and Nairn, 2005). Coseismic landsliding is a possible consequence of both syn-eruptive and post-eruption seismicity; earthquakes larger than ~ M_W 6 or so are known to be capable of causing landslides (Hancox et al., 1995) and, depending on the seismic time-series generated over the study period, may have significant impacts on rivers where they run through steep terrain.

6.2 Initial trigger: Okataina eruption

The volcanic scenario is loosely based on an interpretation (Todde et al., in press) of the Kaharoa eruption as a long-duration, low-intensity but large-volume eruption. This will consist of multiple explosive vent openings followed by dome-building episodes over a period of several years.

6.2.1 Eruption progression

The specific eruptive state of the volcano over time will be based on the intra-eruption (phases) model of Bebbington and Jenkins (2019), updated with additional historical (Bebbington and Jenkins, in preparation) and geological information (Bonadonna et al., 2005; Nairn et al., 2001; Sahetapy-Engel et al., 2014). The model uses a Markov chain to control transitions between the following phase types: effusive (Eff), effusive and explosive (Eff+Exp), continuously explosive (Cts Exp), intermittently explosive (Int Exp), minor explosion (Min Exp), minor eruption (Min Erup), major eruption (Maj Erup) and Plinian eruption (Plinian Erup).

There are only 19 rhyolitic eruptions in the historical database, insufficient for a robust model. Instead we will see our model using all rhyolitic, dacitic and trachyte (high SiO_2) eruptions (80 total) in the historical database. This yields the transition matrix shown in Table 2:

Table 2. Transition matrix for rhyolitic, dacitic and trachyte eruptions in the historical eruption record. The current eruption state is the row, and columns indicate probability of the next eruptive state, conditional on the current (row).

	Eff	Eff +Exp	Cts Exp	Int Exp	Min Exp	Min Erup	Maj Erup	Plinian Erup	End
Start	0.01	0.14	0.03	0.40	0.09	0.21	0.06	0.06	0
Eff	0.40	0.10	0	0.13	0.03	0.13	0.03	0	0.2 0
Eff+Exp	0.10	0.17	0.02	0.29	0	0.05	0.05	0	0.3 2
Cts Exp	0.17	0.08	0	0.50	0	0.25	0	0	0
Int Exp	0.09	0.14	0.09	0.18	0.01	0.05	0.02	0.02	0.4 0
Min Exp	0.10	0.10	0	0.20	0.10	0	0	0	0.5 0
Min Erup	0.09	0.02	0.02	0.22	0	0.27	0	0.02	0.3 6
Maj Erup	0.25	0.17	0	0.25	0	0.08	0.08	0.17	0
Plinian Erup	0.08	0.08	0	0.58	0	0	0.08	0.17	0

The transition matrix describes the probabilities of moving from one phase to another. For example, the (estimated) probability of an intermittently explosive phase (Int Exp) being the start of an eruption for all high SiO_2 eruptions in the historical database is 0.4, and the most common phase to occur after an effusive phase (Eff) is another effusive phase. Work is underway to include noise to any collection of phases to improve model robustness, avoiding the zeros in Table 2 resulting from the small data set.

This transition matrix will be adjusted using the geological data to arrive at a longer-duration eruption consistent with the Kaharoa event. Locations of new vents will be along the Tarawera linear vent zone (LVZ), using data from the 1886 eruption for distances along the vent. A new vent is indicated by a major eruption (or larger) following a dome-building phase as this is most likely to reflect the subsurface processes.

6.2.2 Phase parameters

The duration, and duration of following quiescence (if any), of explosive phases as distributions are available from the intra-eruption phase model. For effusive phases, the dome-building durations will be adjusted using the survival model of Wolpert et al. (2016). Models for daily extrusive volumes will be based on data from Montserrat (Ryan et al., 2010) and/or Popocatepetl (Gómez-Vazquez et al., 2016).

Large explosive volumes will be modelled from Sahetapy-Engel et al. (2014), while continuous/intermittent explosive phases will be presumed to consist of discrete explosions with small plume heights (≤ 10 km) and mass concentrated at the top of the plume (i.e. vulcanian). Plume heights will be sampled (following Biass et al., 2016a). The explosion reposes will follow a log-logistic survivor function (Connor et al., 2003), adjusted to approximately hourly frequency (Bebbington and Jenkins, 2019).

The eruption column height for instantaneous eruptions can be estimated using the Mastin et al. (2009) best fit of

$$H = 25.9 + 6.64(V)$$

where H is plume height and V is eruption volume (in km^3 DRE). The mass flow rate will be calculated from plume height (Folch et al., 2020; Mastin et al., 2009), $\dot{V} = 140.8 \cdot H^{4.15}$. The eruption duration can then be estimated by dividing the volume by the mass flow rate.

Models for the occurrence of other volcanic hazards will be developed following Ogburn et al. (2015), based on the DomeHaz (https://vhub.org/groups/domedatabase) database. These will include dome collapses/avalanches. An estimate of block-and-ash flow height exceedance probabilities (conditional on an eruption and dome collapse) can be calculated by sampling an emulator at randomly-drawn dome configurations, with volumes drawn from a power law distribution fitted to the record of dome collapses (Harnett et al., 2019).

6.2.3 Hazard models

Eruption products for the specific eruption state, intensity and volume will be simulated to detail the volume and grain size distribution of tephra in each catchment (or sub-catchment). The three-dimensional advection-diffusion model Fall3D (Folch et al., 2020) will be used to simulate ashfall. The likelihood and volume of column-collapse pyroclastic flows will be derived from the work of Carazzo et al. (2020) and simulated using simple Bernoulli flow models (e.g. Energy Cone; Tierz et al., 2016). High-intensity rainstorms could result in remobilisation of volcaniclastic deposits as lahars. The extent, level of detail and appropriate methodology required to simulate lahar impacts will be investigated during this research.

Other volcanic phenomena that are expected to have a minimal impact on the sediment cascade will be estimated on an as-needed (i.e. impact-led basis using appropriate models (e.g. Biass et al., 2016b for ballistics; Gallant et al., 2018 for lava). Volcanic earthquakes will be based on Sinabung (McCausland et al. 2019), with effects fed through the earthquake model (section 6.3.2).

6.3 Subsequent triggers

6.3.1 Weather sequence

Weather is included in this MRm system both for direct impacts (e.g. wind gusts knocking out powerlines) and for indirect impacts through other modules. Wind parameters influence tephra

distribution, while rainfall amounts, durations and intensities drive erosion, flooding and sedimentation, and inform landslide-triggering equations.

A probabilistic weather model is required that provides realistic wind and rainfall parameters over a 20- to 30-year period at a minimum daily resolution across the region. Wind parameters with height are required above Tarawera vent(s) and for the rest of the Case Study area during eruptive episodes; surface wind velocities may be required for direct wind impacts on infrastructure, and higher temporal resolution rainfall intensities (e.g. for thunderstorms) may be necessary for specific sedimentation, landslide triggering, and/or flooding scenarios.

Weather in New Zealand is driven by the Southern Hemisphere westerly circulation belt with high pressure (anticyclones – little to no rain) migrating across every six to seven days, between which are troughs of low pressure (bringing wind and rain). These translate into surface weather through sea/land interactions with the mountain chain(s) down the centre of NZ having a major influence on regional climate (Lorrey and Bostock, 2017).

Weather in the Bay of Plenty (BoP) is highly variable in both time and space. As in other parts of New Zealand, rainfall distribution closely follows the topography (Chappell, 2014; see Fig. 8 for case study elevations). Across our Case Study, this translates to significantly higher rainfall (more than twice as much) around Tarawera (NW), high rainfall in the Ikawhenua and Huiarua Ranges (E/SE) but much lower in the central area of the catchments (Fig. 12). Seasonal variability is noted in both wind and rain parameters with spring being the windiest season (but with the highest gusts in winter), and the greatest rainfall occurring in winter.

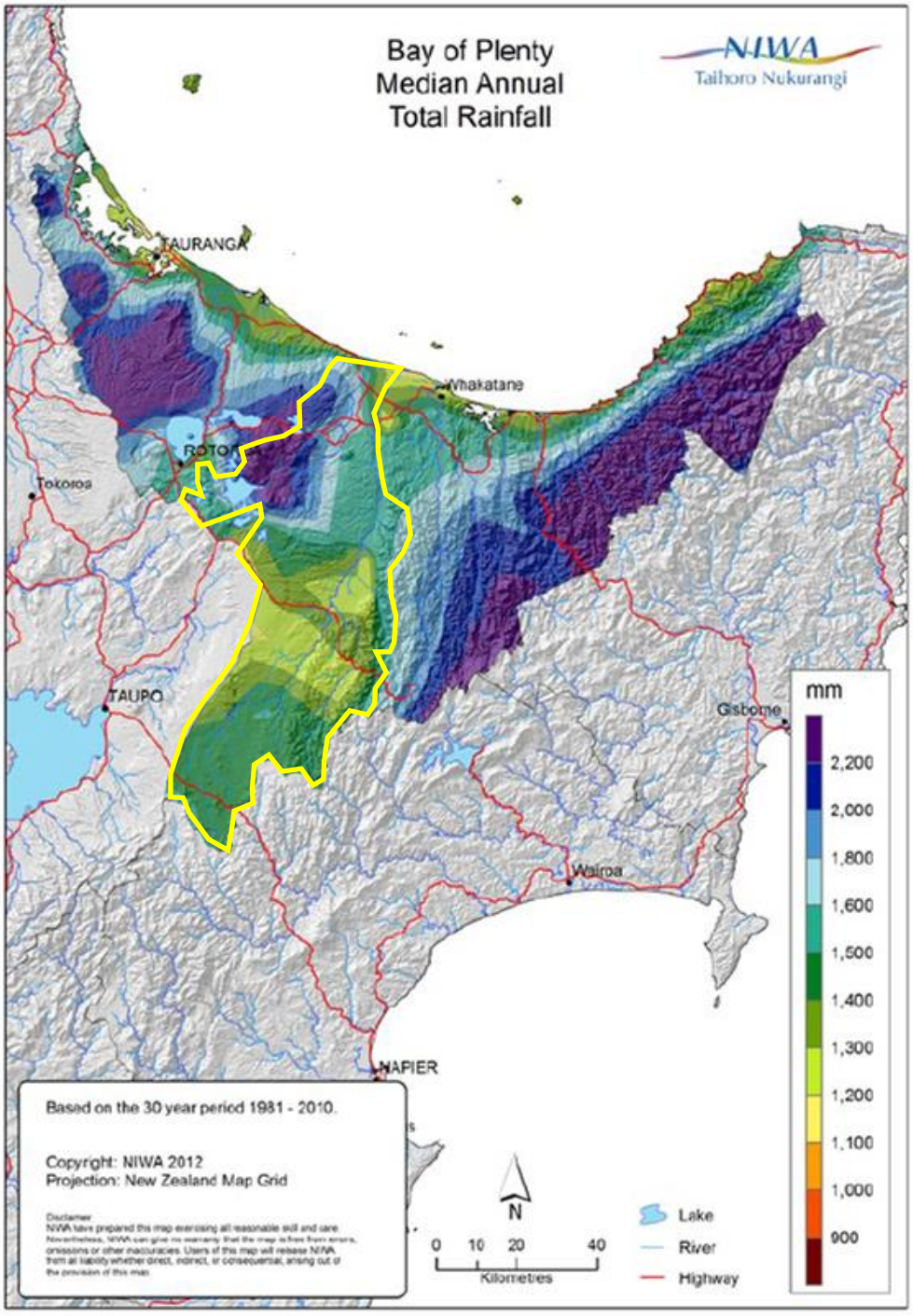

Fig. 12. Median annual total rainfall for Bay of Plenty, 1981 – 2010 (Chapell, 2014) with Case-Study area outlined in yellow.

Convectional precipitation (thunderstorms) can be responsible for the highest hourly and daily totals, and is usually localised rather than widespread (e.g. the Matatā storm 2005, Fig. 13). These convectional storms can be very effective sediment mobilising agents so cannot be overlooked or averaged out via daily or spatially-invariant rainfall totals.

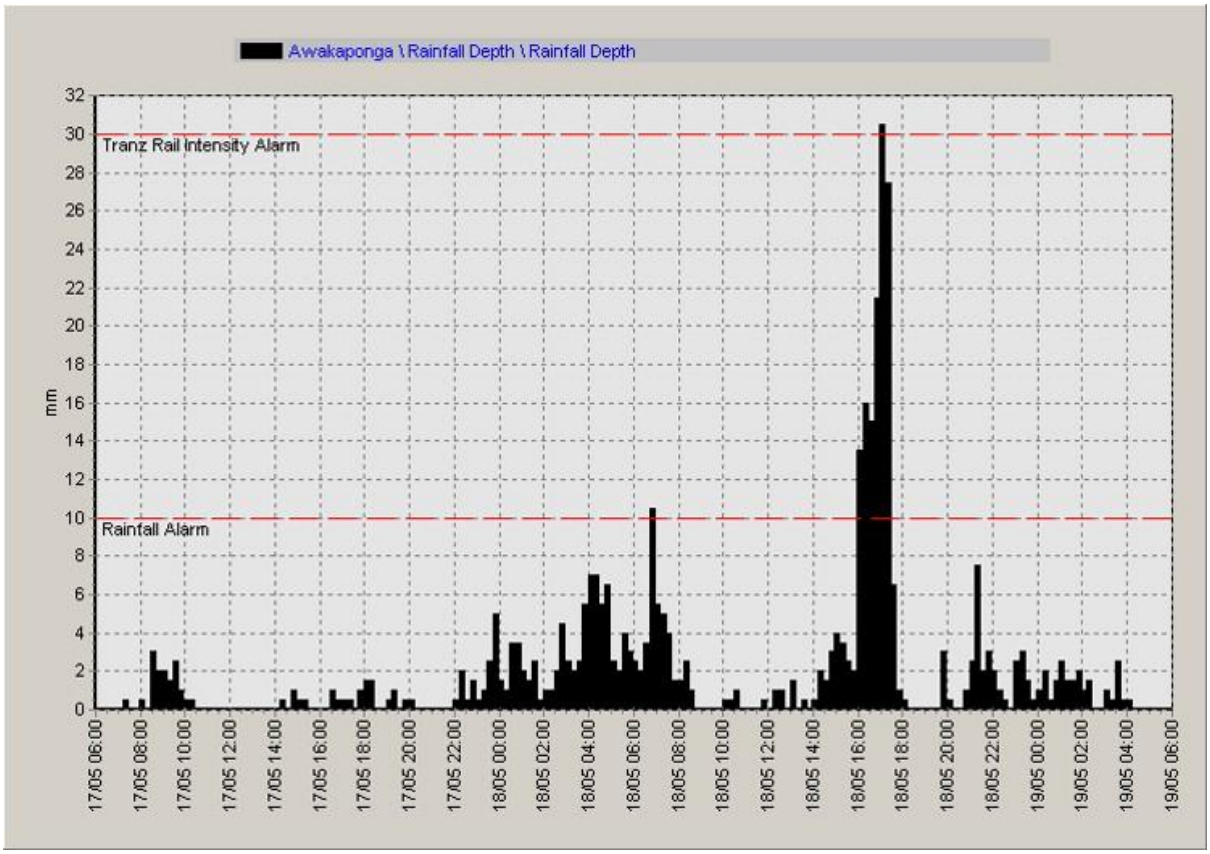

Fig. 13. Histogram of 15-minute rainfall totals at Awakaponga (from Environment-Bay-of-Plenty records) during the Matatā storm. Figure taken directly from McSaveney et al. (2005).

The Case Study area is also located well within the reach of more extreme weather events, namely extra-tropical cyclones (low-pressure rapidly-rotating storm systems). Thus, these should also be included in any long-term weather model due both to their relatively frequent occurrence and their potential for significant direct and indirect impacts on the MRm system. New Zealand is on average hit by slightly more than one tropical storm per year with the greatest number of storms reaching NZ in February and March (Sinclair, 2002). While the paths of extra-tropical cyclones rarely cross the BoP, the accompanying high winds and heavy rainfall frequently affect the Case Study area. For example, ex-tropical cyclone Sose (April 2001) caused heavy rain and flooding across the BoP (Chappell, 2014), cyclone Fergus (December 1996) caused significant road damage, and ex-tropical cyclone Bernie (April 1982) destroyed $1.2 million in kiwifruit crops in the area. Other cyclones that have affected the area in the last 40 years include Cook (April 2017), Debbie (2017), Innis (2009), Ivy (2004), Gavin (1997), and Bola (March 1988) (all cyclone impact information from the NZ Historic Weather Events Catalogue: https://hwe.niwa.co.nz/).

The weather model must accommodate these spatial and seasonal variabilities and explicitly include both convectional storms and ex-tropical cyclones whilst maintaining smooth transitions between time and weather steps.

Daily surface weather data for the Case Study area are available from NIWA either via a virtual climate station paid service created from the interpolation of observed data, or via freely from CliFlo as direct observations (https://cliflo.niwa.co.nz/). Hourly rainfall data are also available but at a significantly reduced spatio-temporal level (Fig. 14). Wind data with height above Tarawera are only available from climate reanalysis datasets (models + data assimilation) as direct observations are limited to surface wind speeds at proximal weather stations (e.g., Rotorua and Whakatane airports). ECMWF v5 (ERA5: https://www.ecmwf.int/en/forecasts/datasets/reanalysis-datasets/era5) provides hourly wind data

over a 30 km spatial grid, 137 atmospheric levels up to 80km and with 'data' from 1979 to present day and associated spatio-temporal uncertainty estimates (Hersbach et al., 2020). ERA5-land reanalysis data provides hourly rainfall data over a 9 km spatial grid with values from 1981 to the present day (Muñoz Sabater, 2019). However, actual rainfall data are not incorporated into the reanalysis set until 2009 (i.e., values before then are purely theoretical) and there are no uncertainty estimates associated with the values provided.

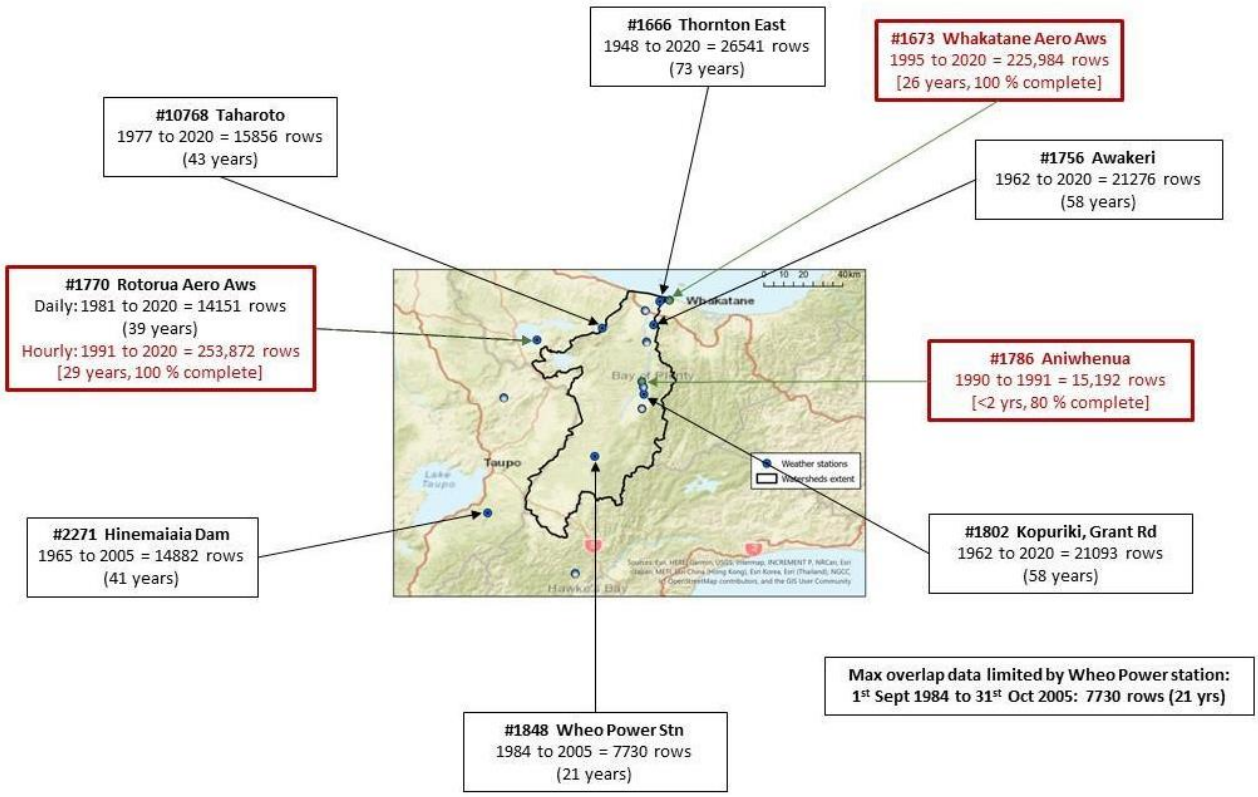

Fig. 14. Daily (black) and hourly (red) rainfall data available from CliFlo for this Case Study

The RNC2 Weather and Wildfire programme (resiliencechallenge.nz/scienceprogrammes/weather-theme/) has completed 36-hour simulations of five ex-tropical cyclones and produced corresponding high-spatiotemporal-resolution weather data (up to 15 minute, 330 m grids; Boutle et al., in prep). Current available outputs are of five events (Cook 2017, Donna 2017, Lusi 2014, Pam 2015, Victor 2016) with six different paths (one control plus five adjusted). Through collaboration with this programme, a total of 30 different datasets are immediately available for direct incorporation into the MRm probabilistic weather model. As more simulations are run, further data will become available for a wider variety of storms thus enriching the tropical cyclone database from which to draw from when including one of these more extreme events.

The probabilistic weather model will follow a "chop and stitch" approach. Daily rainfall data will be chopped into blocks with cut-offs lying in the temporal centre of days of zero rainfall - thus preserving any extended rainfall sequences and ensuring cut-offs are within troughs to maintain local atmospheric circulation parameters. Surface wind direction will be captured at the start and end dates of each block. The start block will be randomly selected (from a multi-year dataset) based on simulation start-date. Weather progression will be based on the random selection of blocks time-stamped (day-month) within a subsequent (or previous) time-period of several weeks from any year within the dataset, thus preserving seasonality. Block selection will also be conditional on the surface

wind direction – subsequent wind start direction must be such that unrealistic shifts in wind direction are avoided.

To incorporate tropical cyclones, the likelihood of a tropical cyclone impacting the area on a given date will be based on a monthly (constant) probability. For example, the probability of a tropical cyclone in November will be significantly less than one occurring in February. A range of values will be used in preliminary runs to determine the most practical set-up with these ranges informed by the RNC2 Weather and Wildfire programme and research on the climatology of tropical storms proximal to New Zealand (e.g. Lorrey et al., 2014; Sharma et al., 2020; Sinclair, 1994). Should a tropical cyclone 'occur', one of the 30 weather datasets from the RNC2 Weather and Wildfire programme will be randomly selected and will supplant any existing weather. After the 36 hours of simulated data, weather will return to the previous block.

As no weather data are created within this model, maximum temporal and spatial resolution is governed entirely by the input data. Standard weather model outputs will be:

(1) daily rainfall totals (mm) at seven pre-defined locations (weather stations) across the Case Study, together with hourly rainfall totals for convective storms
(2) wind velocities (direction and speed) at pre-defined heights (from tephra distribution model requirements) at Tarawera vent – can be reported daily or only when an eruptive episode is occurring,
(3) daily maximum wind gusts if required for direct wind impacts assessment,
(4) hourly wind velocities (surface and with height) and rainfall during any tropical cyclone event at a maximum resolution of 330 m.

These outputs can be expanded without significant alteration to the model as required by the other MRm modules but are limited to available data (and resolutions thereof). An outstanding issue is that of hourly rainfall data. This is only available over any substantial period at two points proximal to our Case Study: Whakatane and Rotorua airports (Fig 14). This will likely form a necessary limitation of the weather model. Data may be imputed across the Case Study by comparison of hourly rainfall values at (and lag between) these stations with daily rainfall totals at these and then the other stations across the region. It is not thought that any bias towards underestimation of convective storm occurrence will be introduced via this process as any thunderstorms should pass over these points however, additional investigations will be carried out to assess the validity of this assumption through the comparison of CliFlo hourly and daily amounts at the stations shown in Fig 14 with sub-hourly data from the telemetered monitoring sites at: https://monitoring.boprc.govt.nz/MonitoredSites/cgi-bin/hydwebserver.cgi/districts/details?district=3 (Environment-Bay of Plenty Live Monitoring site: visualisations of recent data).

6.3.2 Earthquake sequence

Earthquakes produce ground shaking that generally decreases with distance from the epicentre; however, depending on the local ground characteristics at a location of interest, this shaking could be amplified. These earthquakes could be a potential catalyst for other events, e.g. landslide on a hill slope saturated by prolonged recent rainfall events. In this section, we are interested in the spatio-temporal probability of earthquakes that could affect the Case Study region together with the levels of heterogeneous ground shaking across the region (Fig. 15)

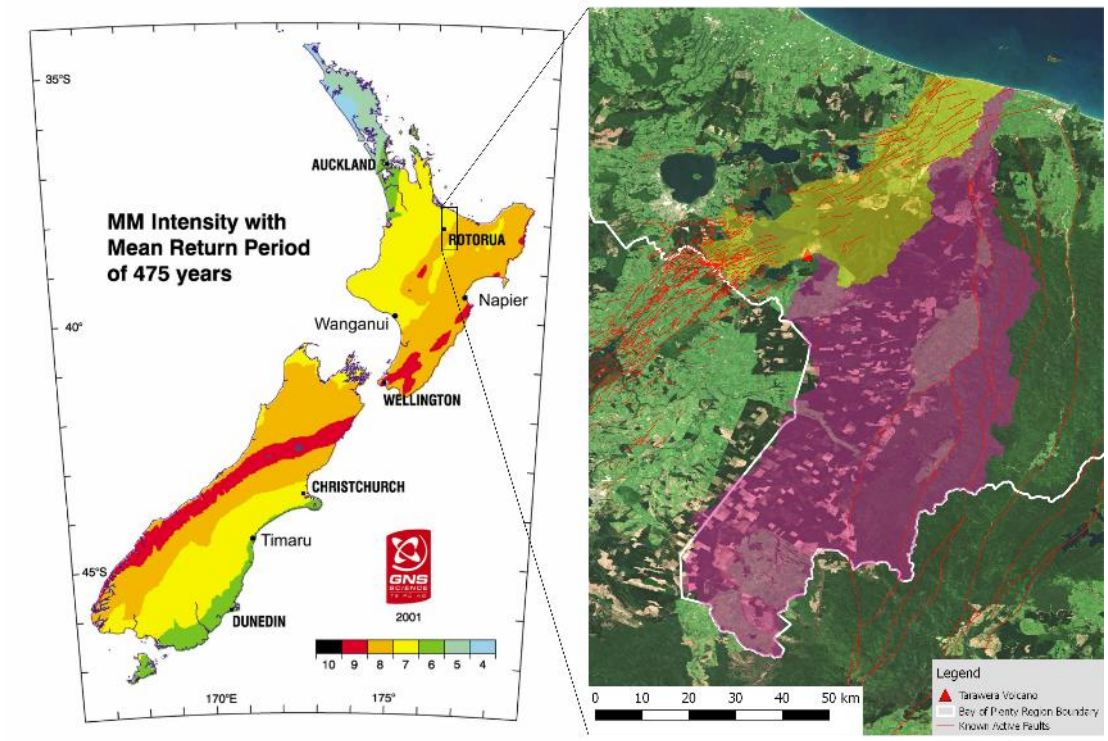

Fig. 15. Left: Seismicity in Case Study area (black square) compared with the rest of NZ (GNS Science Ltd.); Right: Known active faults (red) in the Case Study area (yellow and purple)

We can broadly categorise earthquakes in the Bay of Plenty as tectonic or volcanic. Tectonic events often occur with a relatively large mainshock followed by an aftershock sequence, which continues until the stress regime around the ruptured fault reaches a quasi-stable equilibrium (Bebbington et al. 2016). Approximately 40% of the events in NZ do not obviously belong to a known aftershock sequence and are of small to middling magnitude. However, aftershock sequences can last for many hundreds of years, hence there is some debate about the nature of these small to middling magnitude events. Volcanically-generated earthquake sequences tend to be swarm-like, where the event magnitudes are more similar; the largest event does not generally initiate the sequence, and the events are more compactly distributed in space and time. Volcanic sequences tend to finish rather abruptly whereas aftershock sequences have a very long temporal decay.

The Epidemic Type Aftershock Sequence (ETAS) model (Ogata, 1988; Ogata, 1998) is currently the most successful model for forecasting aftershock sequences (Harte, 2017; Harte, 2019; Omi et al., 2013; Omi et al., 2015; Omi et al., 2016; Omi et al., 2018; https://www.statsresearch.co.nz/dsh/sslib/?examples?forecast). It consists of two additive components: a background term and the triggering or aftershock term. The weak point of this model is the background term: is it essentially a mop-up term for aftershocks of large historical events not contained in the earthquake catalogue, or that these background events simply represent “noise” in the system (hence Poisson in nature) and it is difficult to attribute them to any particular physical process, or a combination of both. This model is used to produce routine earthquake forecasts for NZ by simulating the process forward over the forecast space-time interval, given the observed events up until the start of this interval. Software is written in the R language and controlled by a BASH script, and available on the web (Harte, 2019, suppl. material; https://www.statsresearch.co.nz/dsh/sslib).

The Stress Release Model (SRM) assumes that tectonic stress accumulates over a long period of time, continuing until it reaches a critical threshold, resulting in a large event (Bebbington and Harte, 2003;

Bebbington and Harte, 2001; Lu et al., 1999). This stress build-up can be over centuries and the critical threshold is random in nature; the randomness represents other possible physical influences not accounted for by the model. Hence for its application, there is a minimal requirement of a long historical record of large magnitude events. Ideally, a model of this form should be part of the background term in the ETAS model. This model has been applied in various research studies, but not in a routine forecasting manner like the ETAS model. Software for simulation and fitting is also available on the web (https://www.statsresearch.co.nz/dsh/sslib). The combined SRM/ETAS model will be calibrated against the New Zealand seismic hazard model (Stirling et al., 2012).

Models for volcanic swarms are not so well developed. They appear to be at a magnitude level which may not be damaging in and of themselves, except for possibly large (c. M6) events that occur as part of a fissure eruption (Benoit and McNutt, 1996). Hence, in the main, the swarms potentially provide information on future volcanic activity for management decisions. Our intention is to use a spatial distribution for the study region that represents the relative probabilities of a swarm initiating at a given point. This may be informed by vent migration. We will also assume an initiation rate (non-homogeneous Poisson process) for this region, correlated to the likely next stage of eruption. To simulate, one would sample a time and spatial location from this density and rate. One would then simulate events according to an assumed spatial distribution about the initiation point. The temporal length of the sequence and event magnitudes are also random according to assumed probability distributions based on historical data (Benoit and McNutt, 1996).

The amount of ground shaking felt at a particular location is complex and is related to the ground conditions, including topography (e.g. Buech et al. 2010), at that site. A physical model for such phenomena would be extremely complex, and hence knowledge of this effect is largely based on historical empirical observations. GeoNet collects "Felt" reports from the public (https://www.geonet.org.nz/data/types/felt). This gives a measure of the ground shaking at various locations which can then be related to the magnitude of the given event. However, the sampling intensity is explicitly related to the population density at a given location and self-selection by individuals; but much of our Case Study region is relatively sparsely populated. This bias is further exacerbated by local geophysical characteristics, for example, there will be less people located on steep hill slopes which are prone to induced landslide, and more in river valleys which will have higher levels of ground shaking with, for example, consequential damage to "natural" dams formed by forestry slash after a high rainfall event.

The OpenQuake Project (Pagani et al., 2014) includes attempts (Abbott et al., 2020; Chiou et al., 2010; Chiou and Youngs, 2014) to empirically characterise ground shaking at locations, of specified physical characteristics, a given distance from the earthquake source. We propose to primarily use this information to characterise ground shaking. This can be checked against recent work on broadband shaking (Bradley et al., 2017; Lee et al., 2020), and will be informed by the BoPRC geological maps (e.g., Fig. 10).

Our model will simulate space-time point locations of earthquake events. When a simulated event occurs, a peak ground shaking map for the entire region will be generated. Clearly there is a boundary effect as earthquake events outside the boundary of the study region, but within a band close to the boundary, may cause damaging ground shaking within the study region. Hence, the region of the simulated earthquake events will be a little larger than our study region. Interest will then focus on whether ground shaking exceeds some threshold (possibly stochastic) at various vulnerable locations within the region: critical man-made infrastructure such as dams (https://www.quakecentre.co.nz/news/case-study-effects-1987-edgecombe-earthquake-matahina-__I.11612__N.112) or stopbanks (https://ir.canterbury.ac.nz/handle/10092/15991). Earthquakes can

also generate other natural hazards phenomena which in turn may affect infrastructure, e.g. landslides, or liquefaction (Bastin et al., 2020).

It is possible that a particularly large earthquake may create a fault scarp (Beanland et al., 1989). This can be modelled using (e.g.) the relations in (Bebbington et al., 2016). The introduction of a scarp may affect the sedimentation transport model, if the scarp is not parallel to the main rivers. Its effects on inundation models are much easier to incorporate.

6.3.3 Landslide sequence

The generally flat topography of much of the study area means that landslides can be restricted to specific areas. In particular, the contribution of (small) landslides to the sediment balance will be subsumed in the sedimentation model. We are only interested in landslides where there is a possible impact on sensitive infrastructure, or where a subsequent hazard (e.g., landslide dam or debris flow) could arise. Slope angle is one of many criteria for landslide occurrence and is shown for the Case-Study area in Figure 16. The apparently large landslide-prone area (based purely on slope angle) on the east of the study area is generally of low relief so most landslides will be very small and thus will be contained within the sedimentation model.

For larger landslides, natural areas of interest include the Matahina dam (Fig. 16C), the Rangitaiki river catchment above the dam (Fig 16: B), and certain areas along the Tarawera river (Fig. 16A). The Matahina dam is of particular interest. In addition to electricity generation, it is the primary control on flooding in the lower Rangitaiki. As such, the water level and sediment buildup in the dam are of great importance, and the possibility of landslide induced tsunami may need consideration. Landslides will be either coseismic, modelled by an adaptation of the process in Robinson et al. (2016), or rainfall triggered. In the latter case we will develop a new model based on Monsieurs et al. (2019) and Porta et al. (submitted).

Landscape changes post-eruption will affect landslide generation and size, however incorporating these effects is highly complex and restricted by a lack of data. Rather, landslide volumes will be estimated on a multivariate regression analysis of past landslide volumes in New Zealand, assuming little landscape change. The model will include the location (e.g. material type, slope) and triggering (magnitude, precipitation) factors as independent variables. Landslide runout, and consequent impacts or formation of a landslide dam will be modelled using Flow-R.

Landslide dams will be formed when the dam resulting from the landslide is sufficient to block a waterway, not just divert it. We will assume for simplicity and realism that the critical point for failure is when the dam is first over-topped. This time can be derived from the rainfall models and the stream network in the sedimentation model, and may be a direct output from the latter. At the critical point, the dam will either fail, releasing a debris flood into the sedimentation model, or become a weir. Stability criteria can be extracted from (e.g.) Ermini and Casagli (2003) and/or Shan et al. (2020), and made probabilistic in line with the analysis of Porta et al. (2020). Post-landslide debris flows and lahars, including landslide dam outbreaks, will be simulated on an as-needed basis by the scenarios.

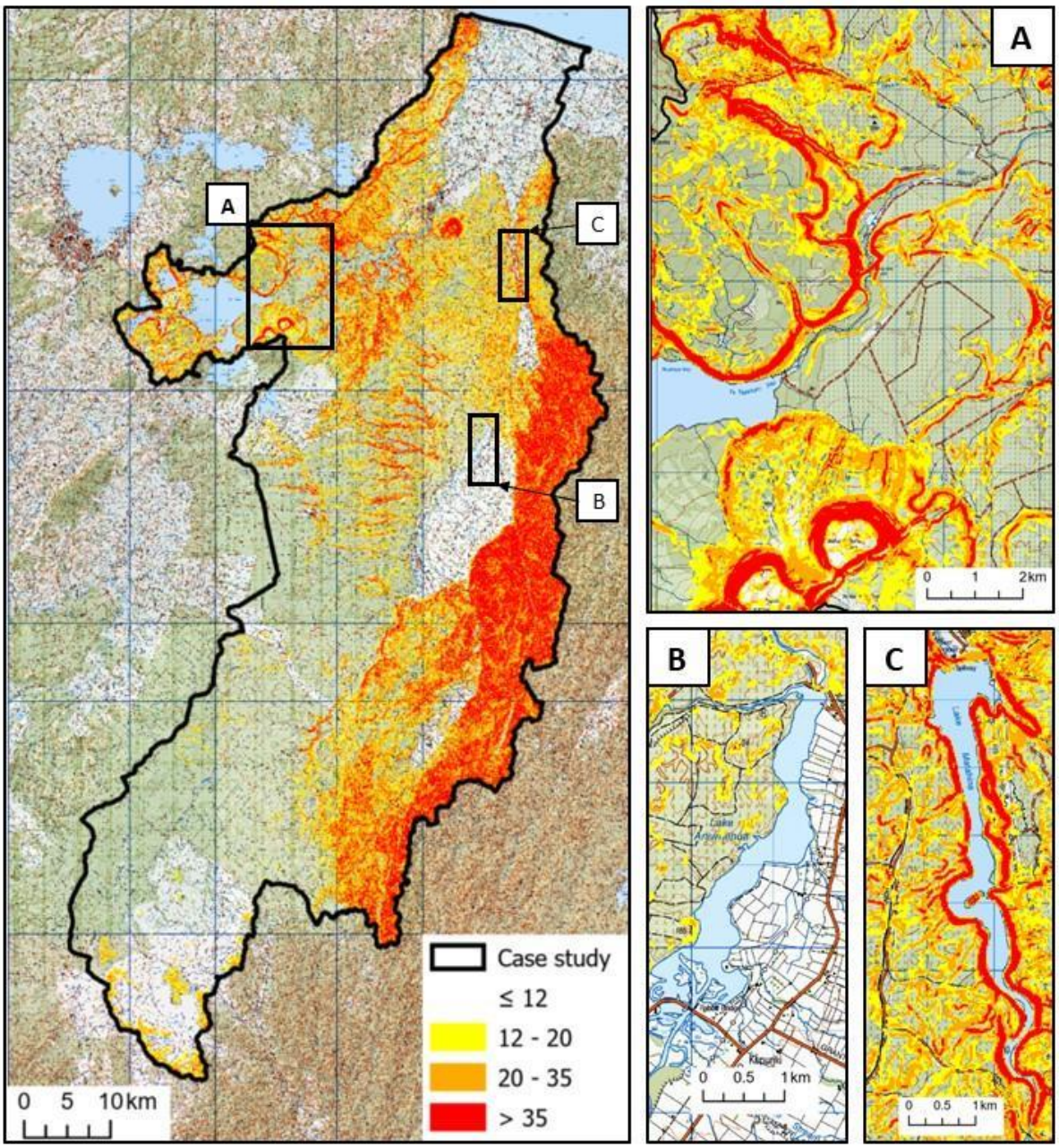

Fig. 16. Slope angle across the area (based on 25 m DEM) on topo50 maps (BE37:BG39), A: Tarawera river, B: Aniwhenua, C: Matahina.

7. Water and sediment transport model

In the MRm case study, a physically-based water and sediment routing model is required to be the engine of the multi-risk model that converts input hazards and decisions into susceptibility and exposure changes that alter impact. Even if a simple one-dimensional sediment transport model is applied to the river network, the Tarawera/Rangitaiki river system is extensive and the catchments cover about 3500 km^2, with about 200 km of main-stem length; when tributaries are included there may be of the order of 1000 km of channel to model. Hence significant simplifications to the field conditions will be needed to constrain the sediment transport model runs to a reasonable computational cost and time-frame.

7.1 Routing model architecture

In detail, a suite of models is to be used in the physical routing model; their integration is illustrated in Fig. 17 and in more detail in Fig. 18. Regardless of the methodology, the class of models suitable for the multi-risk model require a number of relationships as input:

a. Water input to a river reach from land runoff requires a rainfall-runoff sub-model; this will be a function of slope, infiltration and land cover, and will be affected by antecedent soil moisture conditions and eruptive deposition factors (grain size distribution, deposition pattern)
b. Sediment input to a river reach from land runoff requires a rainfall-erosion sub-model, which will be a function of runoff, slope, and sediment density, grading and availability, and is also affected by eruptive deposition factors (grain size distribution, deposition pattern).

These two sub-models will allow the effect of rainfall onto channel-network defined contributing areas in generating both surface runoff and sediment to be quantified as a function of time. Derivation of the relationships underpinning these sub-models (in the context of a tephra landscape) will be the subject of two Masters projects, outlined in Appendix 1.

A hydraulic model will route the sediment and water running off from the landscape down the drainage channel network on a reach-by-reach basis using open-channel hydrodynamics and non-equilibrium sediment transport formulations. Sediment will be routed for multiple size grades and its transport rate will be a function of water flow rate, slope, width and sediment density and grading. As well as outputting water discharge and flow level across the network with time, the model will simulate evolving bed levels due to erosion and deposition (with feedback on flow hydraulics) and will incorporate the effects of anthropogenic structures (e.g., dams and stopbanks). Model application will be the subject of a Masters project outlined in Appendix 1.

A potential hydraulic model (selection to be confirmed) is the CCHE1D model. CCHE1D is a one-dimensional unsteady flow and sediment transport model for channel networks designed to be used in combination with rainfall-runoff and upland erosion models (Viera et al., 2002). CCHE1D's flow module (CCHE1D-FL) computes one-dimensional unsteady flows in dendritic channel networks of arbitrary cross-sectional shapes. Its sediment transport module computes non-equilibrium transport of non-uniform sediment mixtures, which allows the simulation of processes such as hydraulic sorting and armouring, and the determination of changes in bed sediment gradation. Bank toe erosion and bank stability analysis algorithms complement the sediment transport module.

The CCHE1D software and components (shown in Fig. 18) already incorporate terrain and watershed analysis routines to develop a network representation of the watershed-channel system. The channel network model has been integrated with an AGNPS (AGricultural Non-Point Source model, e.g. Bingner, Theurer and Yuan, 2011); this utilizes ephemeral gully evolution capabilities with sheet and rill erosion estimated from the Revised Universal Soil Loss Equation, and provides reach-scale inputs of water and sediment to CCHE1D. CCHE1D is accompanied by a GIS-based graphical interface that facilitates data preparation and manages the integration with other models and tools (Viera et al., 2002).

TopNet will be used as the water-flow component of the AGNPS in this Case Study; it has already been calibrated for the Bay of Plenty region (Singh et al., 2020), and a ready-made erosion and sediment routing module (ESR) will be sought and calibrated to represent the corresponding sediment movement. Note that because of the dominance of volcanic sediments in the existing soils and in the trigger inputs, the hydraulics/sediment transport component of CCHE1D (and AGNPS/ESR) will need

to be modified to account for the different densities of these sediments from those normally used in sediment transport modelling.

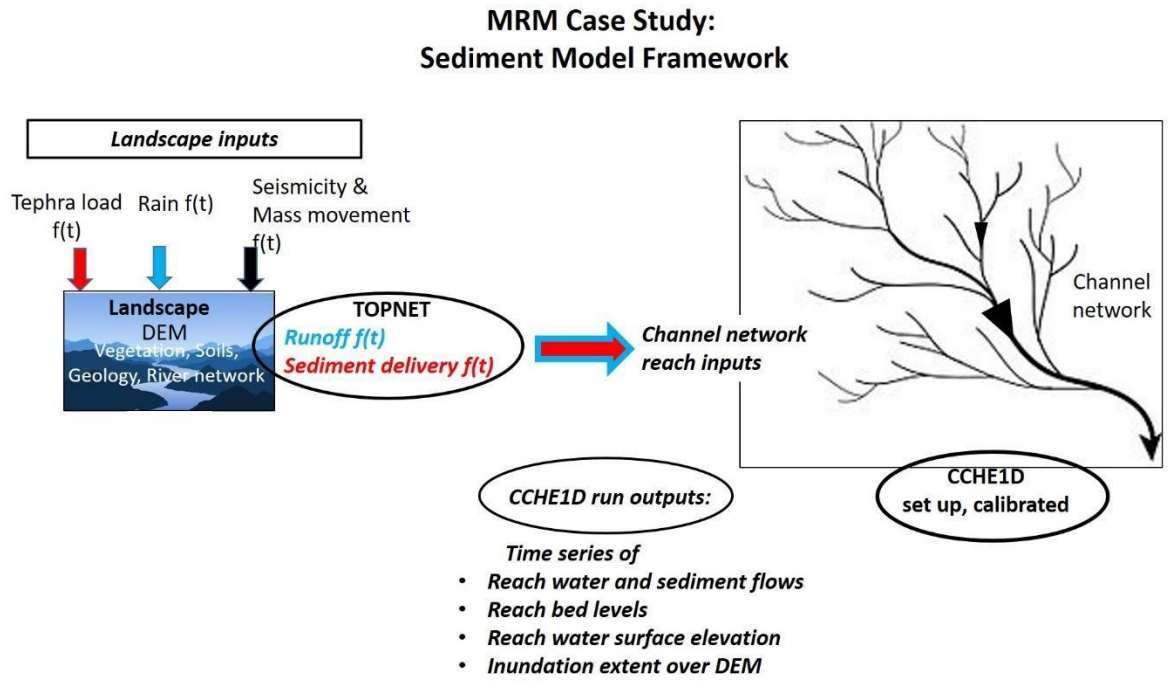

Fig. 17 Sediment model architecture

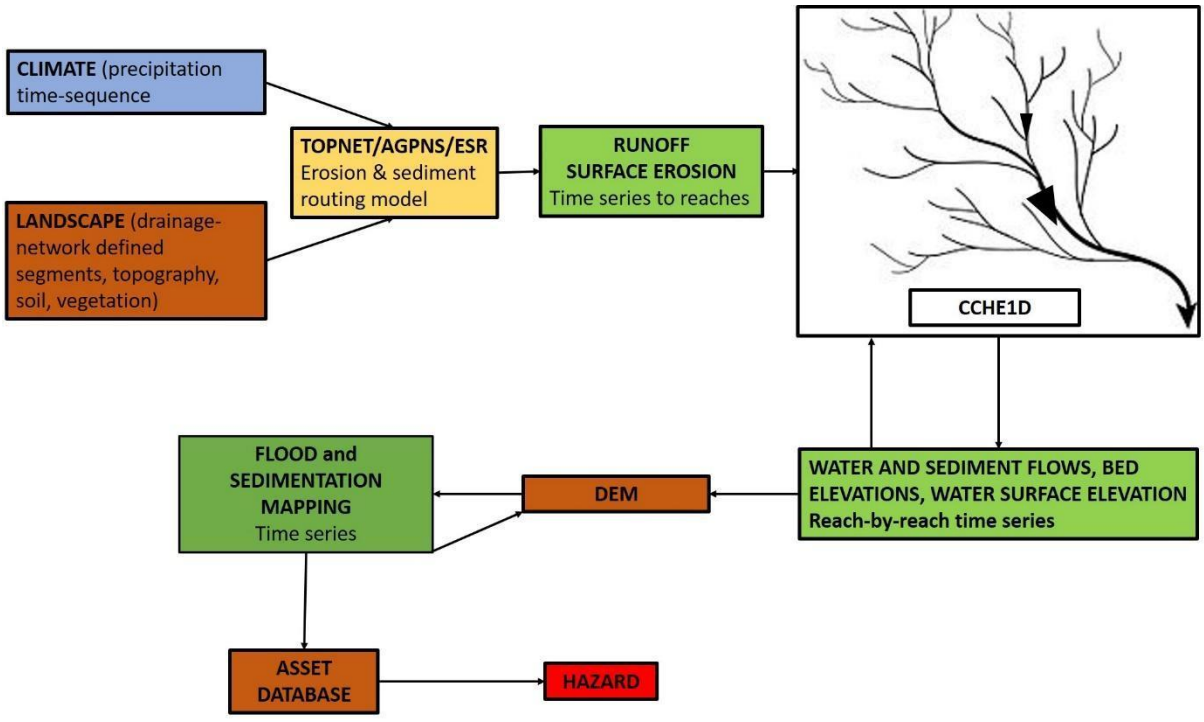

Fig 18. Detail of CCHE1D-based sediment modelling framework and inputs

7.2 Water flow and flooding

The time-sequence of reach water surface levels generated by the hydraulic routing model will allow the extent of flooding to be determined by overlaying these water levels on the digital elevation model

of the areas adjacent to rivers. In particular, increases of river bed level due to sediment deposition will result in higher water surface levels than previously, and the flooding extent corresponding to given water flow rates will alter accordingly.

This increased inundation will affect a wide range of land uses, from agricultural use of soils to functionality of buildings and traffic capacity on roads. In addition, artificial obstacles to water flow such as embankments and stopbanks may fail following earthquakes, when overtopped, or due to seepage, with corresponding redistribution of water and alteration of flood extent.

A consequence of flooding is deposition of sediment on the floodplains, which can also affect land uses and in some cases require removal to restore pre-flood land-use capability. Much of this sediment will be deposited from suspension in slow-moving overbank flood waters; CCHE1D can model this process in the main river channel but an ancillary approximation may need to be developed for representing areally-extensive sedimentation as a function of water depth and time.

7.3 Surface-water groundwater interaction

As noted in 5.1.2. above, the near-surface geology of the Rangitaiki catchment allows a significant proportion of precipitation to infiltrate to the groundwater system, from where it re-emerges farther downstream and much later as exfiltration of groundwater to rivers, mainly under low-flow conditions. This has the effect of reducing flood peaks compared to catchments with similar rainfall but less permeable soils and geology. This interaction is incorporated into the rainfall/runoff sub-model.

Summary

This report outlines the proposed methodology, inputs and inter-connections for physical modelling of a volcanically-triggered hazard cascade leading to flooding impacts and driven, primarily, by long-term sediment aggradation. The model (Fig. 6) consists of exogenous inputs (see section 5) that feed physical process models for volcanic, weather, earthquake and landslide hazards that affect sediment transport and subsequent flood hazards. Each hazard model output also feeds the dynamic impact assessment components of the MRm project to form an end-to-end multihazard risk model.

Future work in the multihazard forecasting component of the MRm theme includes development and implementation of this proposed model (deliverable 2.1.3) and quantification of the physical and socio-economic impacts with the implemented model (deliverable 2.1.4).

Acknowledgements

The ex-Tropical Cyclone inputs are provided by researchers Ian Boutle (visiting scientist to NIWA from the UK Metoffice), and Stuart Moore and Richard Turner of NIWA, who are supported through the Weather and Wildfire programme of Resilience to Nature's Challenges Kia manawaroa – Ngā Ākina o Te Ao Tūroa. The computational facilities for the ex-Tropical cyclone simulations are provided by NeSI and NIWA.

References

Abbott, E., Horspool, N., Gerstenberger, M., Huso, R., Van Houtte, C., McVerry, G. and Canessa, S., 2020. Challenges and opportunities in New Zealand seismic hazard and risk modeling using OpenQuake. Earthquake Spectra, 36(1_suppl): 210-225.

Bastin, S., van Ballegooy, S., Mellsop, N. and Wotherspoon, L., 2020. Liquefaction case histories from the 1987 Edgecumbe earthquake, New Zealand – Insights from an extensive CPT dataset and paleo-liquefaction trenching. Engineering Geology, 271: 105404.

Beanland, S., Berryman, K.R. and Blick, G.H., 1989. Geological investigations of the 1987 Edgecumbe earthquake, New Zealand. New Zealand Journal of Geology and Geophysics, 32(1): 73-91.

Bebbington, M. and Harte, D., 2003. The linked stress release model for spatio-temporal seismicity: formulations, procedures and applications. Geophysical Journal International, 154(3): 925-946.

Bebbington, M., Harte, D. and Williams, C., 2016. Cumulative Coulomb Stress Triggering as an Explanation for the Canterbury (New Zealand) Aftershock Sequence: Initial Conditions Are Everything? Pure and Applied Geophysics, 173(1): 5-20.

Bebbington, M. and Harte, D.S., 2001. On the Statistics of the Linked Stress Release Model. Journal of Applied Probability, 38: 176-187.

Bebbington, M.S. and Jenkins, S.F., 2019. Intra-eruption forecasting. Bulletin of Volcanology, 81(6): 34.

Benoit, J.P and McNutt, S.R., 1996. Global Volcanic Earthquake Swarm Database 1979-1989. USGS Open File Report 96-69.

Biass, S., Bonadonna, C., di Traglia, F., Pistolesi, M., Rosi, M. and Lestuzzi, P., 2016a. Probabilistic evaluation of the physical impact of future tephra fallout events for the Island of Vulcano, Italy. Bulletin of Volcanology, 78(5): 37.

Biass, S., Falcone, J.-L., Bonadonna, C., Di Traglia, F., Pistolesi, M., Rosi, M. and Lestuzzi, P., 2016b. Great Balls of Fire: A probabilistic approach to quantify the hazard related to ballistics — A case study at La Fossa volcano, Vulcano Island, Italy. Journal of Volcanology and Geothermal Research, 325: 1-14.

Bingner, R. L., Theurer, F. D., & Yuan, Y. (2011). AnnAGNPS technical processes: documentation version 5.4. Retrieved from USDA-NRCS website: ftp://ftp.wcc.nrcs.usda.gov/ wntsc/H&H/AGNPS/downloads/AnnAGNPS_Technical_ Documentation.pdf

Blackwood, P., 2000. Review of the flood carrying capacity of the Rangitaiki River below Edgecumbe, Environment BOP.

Bonadonna, C., Connor, C.B., Houghton, B.F., Connor, L., Byrne, M., Laing, A. and Hincks, T.K., 2005. Probabilistic modeling of tephra dispersal: Hazard assessment of a multiphase rhyolitic eruption at Tarawera, New Zealand. Journal of Geophysical Research: Solid Earth, 110(B3).

Boutle, I. A., Moore, S. and Turner, R. (2021). Moving Earth (not heaven): A novel approach to tropical cyclone impact modelling. Weather and Climate Extremes. In prep.

Bradley, B.A., Pettinga, D., Baker, J.W. and Fraser, J., 2017. Guidance on the utilization of earthquake-induced ground motion simulations in engineering practice. Earthquake Spectra, 33(3), pp.809-835.

Briggs, J., Robinson, T. and Davies, T., 2018. Investigating the source of the c. AD 1620 West Coast earthquake: implications for seismic hazards. New Zealand Journal of Geology and Geophysics, 61(3): 376-388.

Britton, R., 2008. Rangitaiki Tarawera Floodplain Management Strategy Stage 1, Environment Bay of Plenty.

Buech. F., Davies, T.R.H. and Pettinga, J.R. (2010). The Little Red Hill Seismic Experimental Study: Topographic Effects on Ground Motion at a Bedrock-Dominated Mountain Edifice. Bulletin of the Seismological Society of America 100: 2219 - 2229

Carazzo, G., Tait, S., Michaud-Dubuy, A., Fries, A. and Kaminski, E., 2020. Transition from stable column to partial collapse during the 79 cal CE P3 Plinian eruption of Mt. Pelée volcano (Lesser Antilles). Journal of Volcanology and Geothermal Research, 392: 106764.

Chappell, P.R., 2014. The climate and weather of Bay of Plenty. NIWA.

Chiou, B., Youngs, R., Abrahamson, N. and Addo, K., 2010. Ground-Motion Attenuation Model for Small-To-Moderate Shallow Crustal Earthquakes in California and Its Implications on Regionalization of Ground-Motion Prediction Models. Earthquake Spectra, 26(4): 907-926.

Chiou, B.S.J. and Youngs, R.R., 2014. Update of the Chiou and Youngs NGA Model for the Average Horizontal Component of Peak Ground Motion and Response Spectra. Earthquake Spectra, 30(3): 1117-1153.

Connor, C.B., Sparks, R.S.J., Mason, R.M., Bonadonna, C. and Young, S.R., 2003. Exploring links between physical and probabilistic models of volcanic eruptions: The Soufrière Hills Volcano, Montserrat. Geophysical Research Letters, 30(13).

Davies, T., Mead, S., Bebbington, M., Dunant, A., Harmsworth, G., Harte, D., Harvey, E., Paulik, R., McDonald, G. and Smith, N., 2020. Multi-Hazard Risk Model, Flooding Case Study: Selection of River System and Potential Hazard Cascades.

Ermini, L. and Casagli, N., 2003. Prediction of the behaviour of landslide dams using a geomorphological dimensionless index. Earth Surface Processes and Landforms, 28(1): 31-47.

Folch, A., Mingari, L., Gutierrez, N., Hanzich, M., Macedonio, G. and Costa, A., 2020. FALL3D-8.0: a computational model for atmospheric transport and deposition of particles, aerosols and radionuclides – Part 1: Model physics and numerics. Geosci. Model Dev., 13(3): 1431-1458.

Gallant, E., Richardson, J., Connor, C., Wetmore, P. and Connor, L., 2018. A new approach to probabilistic lava flow hazard assessments, applied to the Idaho National Laboratory, eastern Snake River Plain, Idaho, USA. Geology, 46(10): 895-898.

Gillon, M. D. (2007). Re-evaluation of internal erosion incidents at Matahina Dam, New Zealand. Internal erosion of dams and their foundations, 115-132.

Gómez-Vazquez, A., De la Cruz-Reyna, S. and Mendoza-Rosas, A.T., 2016. The ongoing dome emplacement and destruction cyclic process at Popocatépetl volcano, Central Mexico. Bulletin of Volcanology, 78(9): 58.

Gran, K.B. and Montgomery, D.R., 2005. Spatial and temporal patterns in fluvial recovery following volcanic eruptions: Channel response to basin-wide sediment loading at Mount Pinatubo, Philippines. GSA Bulletin, 117(1-2): 195-211.

Griffiths, E. (1985). Physical Characteristics of Soils in the Proposed Te Teko and Edgecumbe Irrigation Schemes, Bay of Plenty: N.Z. Soil Bureau District Office, Department of Scientific & Industrial Research.

Hancox, G. T., Perrin, N. D., Dellow, G. D. 1995. Earthquake-induced landsliding in New Zealand and implications for MM intensity and seismic hazard assessment. EQC funded project 95/196

Harnett, C.E., Thomas, M.E., Calder, E.S., Ebmeier, S.K., Telford, A., Murphy, W. and Neuberg, J., 2019. Presentation and analysis of a worldwide database for lava dome collapse events: the Global Archive of Dome Instabilities (GLADIS). Bulletin of Volcanology, 81(3): 1-17.

Harte, D.S., 2017. Probability distribution of forecasts based on the ETAS model. Geophysical Journal International, 210(1): 90-104.

Harte, D.S., 2019. Evaluation of earthquake stochastic models based on their real-time forecasts: a case study of Kaikoura 2016. Geophysical Journal International, 217(3): 1894-1914.

Hersbach, H., Bell, B., Berrisford, P., Hirahara, S., Horányi, A., Muñoz-Sabater, J., Nicolas, J., Peubey, C., Radu, R. and Schepers, D., 2020. The ERA5 global reanalysis. Quarterly Journal of the Royal Meteorological Society, 146(730): 1999-2049.

Hodgson, K. and Nairn, I., 2005. The c. AD 1315 syn-eruption and AD 1904 post-eruption breakout floods from Lake Tarawera, Haroharo caldera, North Island, New Zealand. New Zealand Journal of Geology and Geophysics, 48(3): 491-506.

Kobayashi, T., Nairn, I., Smith, V. and Shane, P., 2005. Proximal stratigraphy and event sequence of the c. 5600 cal. yr BP Whakatane rhyolite eruption episode from Haroharo volcano, Okataina Volcanic Centre, New Zealand. New Zealand Journal of Geology and Geophysics, 48(3): 471-490.

Lee, R.L., Bradley, B.A., Stafford, P.J., Graves, R.W. and Rodriguez-Marek, A., 2020. Hybrid broadband ground motion simulation validation of small magnitude earthquakes in Canterbury, New Zealand. Earthquake Spectra, 36(2), pp.673-699.

Lorrey, A. and Bostock, H., 2017. The climate of New Zealand through the Quaternary, Landscape and Quaternary Environmental Change in New Zealand. Springer, pp. 67-139.

Lorrey, A.M., Griffiths, G., Fauchereau, N., Diamond, H.J., Chappell, P.R. and Renwick, J., 2014. An ex-tropical cyclone climatology for Auckland, New Zealand. International Journal of Climatology, 34(4): 1157-1168.

Lu, C., Harte, D. and Bebbington, M., 1999. A linked stress release model for historical Japanese earthquakes: coupling among major seismic regions. Earth, Planets and Space, 51(9): 907-916.

Major, J.J., Pierson, T.C., Dinehart, R.L. and Costa, J.E., 2000. Sediment yield following severe volcanic disturbance—A two-decade perspective from Mount St. Helens. Geology, 28(9): 819-822.

Manville, V., Newton, E.H. and White, J.D.L., 2005. Fluvial responses to volcanism: resedimentation of the 1800a Taupo ignimbrite eruption in the Rangitaiki River catchment, North Island, New Zealand. Geomorphology, 65(1): 49-70.

Mastin, L.G., Guffanti, M., Servranckx, R., Webley, P., Barsotti, S., Dean, K., Durant, A., Ewert, J.W., Neri, A., Rose, W.I., Schneider, D., Siebert, L., Stunder, B., Swanson, G., Tupper, A., Volentik, A. and Waythomas, C.F., 2009. A multidisciplinary effort to assign realistic source parameters to models of volcanic ash-cloud transport and dispersion during eruptions. Journal of Volcanology and Geothermal Research, 186(1): 10-21.

McSaveney, M. J., Beetham, R. D., & Leonard, G. S. (2005). The 18 May 2005 debris flow disaster at Matata: Causes and mitigation suggestions. Client Report, 71.

Monsieurs, E., Dewitte, O. and Demoulin, A., 2019. A susceptibility-based rainfall threshold approach for landslide occurrence. Natural Hazards and Earth System Sciences, 19: 775-789.

Muñoz Sabater, J., (2019): ERA5-Land hourly data from 1981 to present. Copernicus Climate Change Service (C3S) Climate Data Store (CDS). (Accessed: November 2020), 10.24381/cds.e2161bac

Nairn, I.A., Self, S., Cole, J.W., Leonard, G.S. and Scutter, C., 2001. Distribution, stratigraphy, and history of proximal deposits from the c. AD 1305 Kaharoa eruptive episode at Tarawera Volcano, New Zealand. New Zealand Journal of Geology and Geophysics, 44(3): 467-484.

Ogata, Y., 1988. Statistical Models for Earthquake Occurrences and Residual Analysis for Point Processes. Journal of the American Statistical Association, 83(401): 9-27.

Ogata, Y., 1998. Space-Time Point-Process Models for Earthquake Occurrences. Annals of the Institute of Statistical Mathematics, 50(2): 379-402.

Ogburn, S.E., Loughlin, S.C. and Calder, E.S., 2015. The association of lava dome growth with major explosive activity (VEI ≥ 4): DomeHaz, a global dataset. Bulletin of Volcanology, 77(5): 40.

Omi, T., Ogata, Y., Hirata, Y. and Aihara, K., 2013. Forecasting large aftershocks within one day after the main shock. Scientific Reports, 3(1): 2218.

Omi, T., Ogata, Y., Hirata, Y. and Aihara, K., 2015. Intermediate-term forecasting of aftershocks from an early aftershock sequence: Bayesian and ensemble forecasting approaches. Journal of Geophysical Research: Solid Earth, 120(4): 2561-2578.

Omi, T., Ogata, Y., Shiomi, K., Enescu, B., Sawazaki, K. and Aihara, K., 2016. Automatic Aftershock Forecasting: A Test Using Real-Time Seismicity Data in Japan. Bulletin of the Seismological Society of America, 106(6): 2450-2458.

Omi, T., Ogata, Y., Shiomi, K., Enescu, B., Sawazaki, K. and Aihara, K., 2018. Implementation of a Real-Time System for Automatic Aftershock Forecasting in Japan. Seismological Research Letters, 90(1): 242-250.

Pagani, M., Monelli, D., Weatherill, G., Danciu, L., Crowley, H., Silva, V., Henshaw, P., Butler, L., Nastasi, M. and Panzeri, L., 2014. OpenQuake engine: an open hazard (and risk) software for the global earthquake model. Seismological Research Letters, 85(3): 692-702.

Pain, C.F. and Pullar, W.A., 1968. Chronology of fans and terraces in the Galatea Basin.

Phillips, C. J. 1980: Hydrology and sedimentology of an artificial lake — Lake Matahina, New Zealand. Unpublished MSc thesis, University of Waikato, Hamilton, New Zealand.

Phillips, C.J. and Nelson, C.S., 1981. Sedimentation in an artificial lake-Lake Matahina, Bay of Plenty. *New Zealand journal of marine and freshwater research*, 15(4), pp.459-473.

Pierson, T.C., Major, J.J., Amigo, Á. and Moreno, H., 2013. Acute sedimentation response to rainfall following the explosive phase of the 2008–2009 eruption of Chaitén volcano, Chile. Bulletin of Volcanology, 75(5): 1-17.

Porta, G.F., Bebbington, M., Jones, G. and Xiao, X., 2020. Bayesian lifetime analysis for landslide dams. Landslides, 17, 1835-1848.

Porta, G.F., Bebbington, M., Jones, G. and Xiao, X., submitted. A statistical hazard model for earthquake and/or rainfall triggered landslides. Frontiers in Earth Science.

Robinson, T.R. and Davies, T.R.H., 2013. Potential geomorphic consequences of a future great (Mw = 8.0+) Alpine Fault earthquake, South Island, New Zealand. Nat. Hazards Earth Syst. Sci., 13(9): 2279-2299.

Robinson, T.R., Davies, T.R.H., Wilson, T.M. and Orchiston, C., 2016. Coseismic landsliding estimates for an Alpine Fault earthquake and the consequences for erosion of the Southern Alps, New Zealand. Geomorphology, 263: 71-86.

Robinson, T.R., Rosser, N.J., Davies, T.R.H., Wilson, T.M. and Orchiston, C., 2018. Near-Real-Time Modeling of Landslide Impacts to Inform Rapid Response: An Example from the 2016 Kaikōura, New Zealand, Earthquake. Bulletin of the Seismological Society of America, 108(3B): 1665-1682.

Ryan, G.A., Loughlin, S.C., James, M.R., Jones, L.D., Calder, E.S., Christopher, T., Strutt, M.H. and Wadge, G., 2010. Growth of the lava dome and extrusion rates at Soufrière Hills Volcano, Montserrat, West Indies: 2005–2008. Geophysical Research Letters, 37(19).

Sahetapy-Engel, S., Self, S., Carey, R.J. and Nairn, I.A., 2014. Deposition and generation of multiple widespread fall units from the c. AD 1314 Kaharoa rhyolitic eruption, Tarawera, New Zealand. Bulletin of Volcanology, 76(8): 836.

Shan, Y., Chen, S. and Zhong, Q., 2020. Rapid prediction of landslide dam stability using the logistic regression method. Landslides, 17(12), pp.2931-2956.

Sharma, K.K., Magee, A.D. and Verdon-Kidd, D.C., 2020. Variability of southwest Pacific tropical cyclone track geometry over the last 70 years. International Journal of Climatology, n/a(n/a).

Sinclair, M.R., 1994. An objective cyclone climatology for the Southern Hemisphere. Monthly Weather Review, 122(10): 2239-2256.

Sinclair, M.R., 2002. Extratropical Transition of Southwest Pacific Tropical Cyclones. Part I:Climatology and Mean Structure Changes. Monthly Weather Review, 130(3): 590-609.

Singh, S.K., Augas, J., Pahlow, M. and Graham, S.L., 2020. Methods for regional calibration-a case study using the TopNet hydrological model for the Bay of Plenty region, New Zealand. *Australasian Journal of Water Resources*, pp.1-14.

Snelder, T., Biggs, B. and Weatherhead, M., 2010. New Zealand river environment classification user guide. Ministry for the Environment.

Stirling, M., McVerry, G., Gerstenberger, M., Litchfield, N., Van Dissen, R., Berryman, K., Barnes, P., Wallace, L., Villamor, P. and Langridge, R., 2012. National seismic hazard model for New Zealand: 2010 update. Bulletin of the Seismological Society of America, 102(4): 1514-1542.

Tierz, P., Sandri, L., Costa, A., Zaccarelli, L., Di Vito, M.A., Sulpizio, R. and Marzocchi, W., 2016. Suitability of energy cone for probabilistic volcanic hazard assessment: validation tests at Somma-Vesuvius and Campi Flegrei (Italy). Bulletin of Volcanology, 78(11): 79.

Todde, A., Kereszturi, G. and Procter, J., in press. Stratigraphy and deposit characteristics of the AD1314 Kaharoa eruption at Tarawera, New Zealand - Insights into multiphase rhyolitic eruptions.

Vieira, D.A., Wu, W. and Wang, S.S., 2002, September. Modeling hydrodynamics and channel morphology using CCHE1D. In *Advances in Hydroscience and Engineering, Proceedings of the Fifth International Conference on Hydroscience and Engineering, Warsaw, Poland*.

Wallace, J., Male, J. and Astudillo, J., 2012. Rangitaiki River Modelling Report. 42070518, URS.

Wolpert, R.L., Ogburn, S.E. and Calder, E.S., 2016. The longevity of lava dome eruptions. Journal of Geophysical Research: Solid Earth, 121(2): 676-686.

APPENDIX 1: proposed MSc projects

It has proved to be unfeasible to organise funding for the hoped-for PhD project for the Physical model component of the case study. Instead 3 MSc projects are proposed:

RNC2 MRM MSc project 1 outline

Thesis topic: Rainfall – runoff – erosion relationships for recently-deposited tephra on grassland in North Island, NZ

Supervisor: Stuart Mead, Christian Zammit

Goal: Generate a model to predict runoff from, and erosion of recently-deposited tephra from grassland under given rainfall sequence on a given slope, and delivery sequence to stream.

Objectives:

1. Literature search for field data (e.g. Mt St Helens, Pinatubo, Chaiten); laboratory data; theoretical/numerical models.
2. Assess data for tephra characteristics comparability to NZ
3. Develop numerical rainfall – runoff – erosion code compatible with CCHE1D

References:

Baumann, V., Bonadonna, C., Cuomo, S. and Moscariello, M., 2020. Modelling of erosion processes associated with rainfall-triggered lahars following the 2011 Cordon Caulle eruption (Chile). *Journal of Volcanology and Geothermal Research*, *390*, p.106727.

Korup, O., Seidemann, J. and Mohr, C.H., 2019. Increased landslide activity on forested hillslopes following two recent volcanic eruptions in Chile. *Nature Geoscience*, *12*(4), pp.284-289.

Collins, B.D. and Dunne, T., 2019. Thirty years of tephra erosion following the 1980 eruption of Mount St. Helens. *Earth Surface Processes and Landforms*, *44*(14), pp.2780-2793.

Yang, J., McMillan, H. and Zammit, C., 2017. Modeling surface water–groundwater interaction in New Zealand: model development and application. *Hydrological Processes*, *31*(4), pp.925-934.

Jones, R., Thomas, R.E., Peakall, J. and Manville, V., 2017. Rainfall-runoff properties of tephra: Simulated effects of grain-size and antecedent rainfall. *Geomorphology*, *282*, pp.39-51.

Pierson, T.C., Major, J.J., Amigo, A. and Moreno, H., 2013. Acute sedimentation response to rainfall following the explosive phase of the 2008–2009 eruption of Chaitén volcano, Chile. *Bulletin of Volcanology*, *75*(5), p.723.

Major, J.J. and Mark, L.E., 2006. Peak flow responses to landscape disturbances caused by the cataclysmic 1980 eruption of Mount St. Helens, Washington. *Geological Society of America Bulletin*, *118*(7-8), pp.938-958.

Major, J.J. and Yamakoshi, T., 2005. Decadal-scale change of infiltration characteristics of a tephra-mantled hillslope at Mount St Helens, Washington. *Hydrological Processes: An International Journal*, *19*(18), pp.3621-3630.

Manville, V., Segschneider, B. and White, J.D.L., 2002. Hydrodynamic behaviour of Taupo 1800a pumice: implications for the sedimentology of remobilized pyroclasts. *Sedimentology*, *49*(5), pp.955-976.

Leavesley, G.H., Lusby, G.C. and Lichty, R.W., 1989. Infiltration and erosion characteristics of selected tephra deposits from the 1980 eruption of Mount St. Helens, Washington, USA. *Hydrological sciences journal*, *34*(3), pp.339-353.

Collins, B.D. and Dunne, T., 1988. Effects of forest land management on erosion and revegetation after the eruption of Mount St. Helens. *Earth Surface Processes and Landforms*, *13*(3), pp.193-205.

RNC2 MRM MSc project 2 outline

Thesis topic: Rainfall – runoff – erosion relationships for recently-deposited tephra under forest cover in New Zealand

Supervisor: Tim Davies, Tom Wilson

Goal: Develop a conceptual model to show how runoff from, and erosion of, recently-deposited tephra under forest (exotic and indigenous) differs from that of similar deposits on grassland, including the time-varying impacts of the tephra fall on the forest structure.

Objectives:

1. Literature search for field data (e.g. Mt St Helens, Pinatubo, Chaiten); laboratory data; theoretical/numerical models.
2. Assess data for tephra and forest characteristics comparability to NZ.
3. Develop model relating change in runoff and erosion to time since eruption.

References:

Zobel, D.B. and Antos, J.A., 2017. Community reorganization in forest understories buried by volcanic tephra. *Ecosphere*, *8*(12), p.e02045.

Swanson, F.J., Jones, J., Crisafulli, C., González, M.E. and Lara, A., 2016. Puyehue-Cordón Caulle eruption of 2011: tephra fall and initial forest responses in the Chilean Andes. *Bosque*, *37*(1), pp.85-96.

Németh, K. and Cronin, S.J., 2007. Syn-and post-eruptive erosion, gully formation, and morphological evolution of a tephra ring in tropical climate erupted in 1913 in West Ambrym, Vanuatu. *Geomorphology*, *86*(1-2), pp.115-130.

Antos, J.A. and Zobel, D.B., 2005. Plant responses in forests of the tephra-fall zone. In *Ecological responses to the 1980 eruption of Mount St. Helens* (pp. 47-58). Springer, New York, NY.

Giles, T.M., Newnham, R.M., Lowe, D.J. and Munro, A.J., 1999. Impact of tephra fall and environmental change: a 1000 year record from Matakana Island, Bay of Plenty, North Island, New Zealand. *Geological Society, London, Special Publications*, *161*(1), pp.11-26.

Wilmshurst, J.M., McGlone, M.S. and Partridge, T.R., 1997. A late Holocene history of natural disturbance in lowland podocarp/hardwood forest, Hawke's Bay, New Zealand. *New Zealand Journal of Botany*, *35*(1), pp.79-96.

Collins, B.D. and Dunne, T., 1988. Effects of forest land management on erosion and revegetation after the eruption of Mount St. Helens. *Earth Surface Processes and Landforms*, *13*(3), pp.193-205.

Collins, B.D., Dunne, T. and Lehre, A.K., 1983. Erosion of tephra-covered hillslopes north of Mount St. Helens, Washington: May 1980–May 1981. *Zeitschrift für Geomorphologische Naturwissenschaftliche Forschung*, *16*(1), pp.103-121.

RNC2 MRM MSc project 3 outline

Thesis topic: Modelling volcanic sediment transfer through a fluvial system.

Supervisor: Tim Davies, Stuart Mead, Alex Dunant and Murray Hicks (NIWA).

Goal: To develop and test a one-dimensional model for routing eroded tephra through a fluvial system from the headwaters to the sea, with consideration of aggradation.

Objectives:

1. Become familiar with the models Topnet and CCHE1D and their potential application to the Rangitaiki-Tarawera river systems.
2. Investigate how varying sediment grain density as a function of grain size will affect the sediment transport relationships in CCHE1D.
3. Build, run-in, and calibrate a baseline morphological model of the Rangitaiki fed by an upstream catchment runoff and erosion model for the Kaharoa eruption conditions.
4. Summarise the aggradation/flooding impacts of this event.

References:

Alexander, J., Barclay, J., Sušnik, J., Loughlin, S.C., Herd, R.A., Darnell, A. and Crosweller, S., 2010. Sediment-charged flash floods on Montserrat: the influence of synchronous tephra fall and varying extent of vegetation damage. *Journal of Volcanology and Geothermal Research*, *194*(4), pp.127-138.

Manville, V., Németh, K. and Kano, K., 2009. Source to sink: a review of three decades of progress in the understanding of volcaniclastic processes, deposits, and hazards. *Sedimentary Geology*, *220*(3-4), pp.136-161.

Vieira, D.A., 2006. Modeling hydrodynamics, channel morphology, and water quality using CCHE1D. In *Proceedings of US-China Workshop on Advanced Computational Modelling in Hydroscience and Engineering. Oxford, Mississippi, USA* (pp. 1-13).

Favalli M, Pareschi MT, Zanchetta G. 2006. Simulation of syn-eruptive floods in the circumvesuvian plain (southern Italy). Bulletin of volcanology. 2006 Feb 1;68(4):349-62

Todesco, M., 2004. Volcanic eruption induced floods. A rainfall-runoff model applied to the Vesuvian region (Italy). *Natural hazards*, *33*(2), pp.223-245.

Hayes, S.K., Montgomery, D.R. and Newhall, C.G., 2002. Fluvial sediment transport and deposition following the 1991 eruption of Mount Pinatubo. *Geomorphology*, *45*(3-4), pp.211-224.

.